# Polarizable particles in cavity QED generated time dependent potentials

A masterthesis submitted to the
FACULTY OF
MATHEMATICS, COMPUTER SCIENCE AND PHYSICS,
OF THE LEOPOLD-FRANZENS UNIVERSITY OF INNSBRUCK,

in partial fulfillment
of the requirements for the degree of

MASTER OF NATURAL SCIENCE
(MAGISTER RERUM NATURALIUM)

carried out at the Institute of Theoretical Physics
under the guidance of Dr. Claudiu Genes and Prof. Dr. Helmut Ritsch

presented by
TORSTEN HINKEL

JANUARY 2015

# Contents


**1 Introduction** **1**

**2 Cavity QED with moving atoms** **3**
2.1 Optical cavities and quantized electromagnetic field . . . . . 3
2.2 Atom-light interaction . . . . . 4
2.3 Cavity cooling . . . . . 6
2.4 Doubly pumped cavity . . . . . 8
2.5 Master equation approach . . . . . 9
2.6 Quantum Langevin approach . . . . . 10

**3 Simulation of a quasi-random walk** **11**
3.1 Classical limit with a weakly-driven atom . . . . . 11
3.2 Trajectories and potentials . . . . . 12

**4 Basic concepts of the one dimensional random walk** **16**
4.1 Binomial and Gaussian distribution . . . . . 16
4.2 Drift-diffusion equation . . . . . 17
4.3 Langevin theory of Brownian motion . . . . . 18

**5 Analytical results** **21**
5.1 Dispersive limit . . . . . 21
5.2 Bad cavity limit . . . . . 23
5.3 Steady-state forces . . . . . 23
5.4 Reduction to a perturbed oscillator . . . . . 25
5.5 Simplified model without back-action . . . . . 26

**6 Numerical results** **28**
6.1 Comparison with analytical solutions . . . . . 28
6.2 Discretization of a single trajectory . . . . . 30
6.3 Many trajectories statistics . . . . . 32
6.4 Diffusion for non delta-correlated forces . . . . . 35

**7 Model extensions** **37**
7.1 Saturated single atom . . . . . 37
7.2 Doped nanoparticles . . . . . 38
7.3 Frequency comb driving . . . . . 39

**8 Conclusion and outlook** **43**
8.1 Implementation considerations . . . . . 44
8.2 Applicability for the quantum random walk . . . . . 44

**Bibliography** **47**

# Abstract

We consider the time dependent dynamics of an atom in a two-color pumped cavity, longitudinally through a side mirror and transversally via direct driving of the atomic dipole. The beating of the two driving frequencies leads to a time dependent effective optical potential that forces the atom into a non-trivial motion, strongly resembling a discrete random walk behavior between lattice sites. We provide a general analytical description of the model within the framework of quantum optics before we go to a simplified classical description that relates our problem to the field of nonlinear dynamics. Our numerical investigations provide statistical analysis of the observed quasi-random walk and a comparison of the results with those of Brownian motion. Furthermore we discuss possible extensions of the model towards optomechanics with doped sub-micron particles, realization of a quantum walk with quantum emitters and frequency comb driving.

# Acknowledgements

I acknowledge the support of my family through all the years of study. Also I want to thank my girlfriend for her support and for getting my mind off physical problems when I could not come to an end on my own. It was a great pleasure to work in the research group of Prof. Ritsch and I want to thank him and all group members for the inspiring talks and helpful advices. Especially I am very thankful for the opportunity to join the summer-school in Japan in September last year. At last I want to thank Claudiu. It was a great pleasure to work with him and he was simply the best supervisor i could possibly imagine.

# Chapter 1

# Introduction

Over the past few decades, the optical control of motional degrees of freedom has seen great progress both on the experimental and theoretical fronts. As a particular example of such achievement, the cavity QED setting provides a paradigm for the observation and manipulation of motion of atoms, ions or atomic ensembles via tailored cavity modes. In such a system, the time delay between the action of the field onto the atomic system's motion via the induced optical potential and the back-action of the particle's position change onto the cavity field leads to effects such as cooling or self-oscillations .

The quantum theory of laser cooling [1, 2], the ability of real-time observation of the interaction energy between single atoms and optical cavities [3] and the theoretical investigations of the mechanical effects of optical potentials in resonantly driven cavities on the atomic motion [4] lead the way to investigations on cavity assisted laser-cooling [5]. The friction effect that the atom feels while passing through the cavity field can be explained in the dressed-state picture with a Sisyphus-Cooling mechanism. Analytical expressions for the friction coefficients and momentum diffusion were found for the single particle [6, 8] and many particle case [7]. Many coherently driven atoms inside a cavity field also feature self-organization [9]. The combination of longitudinal and transverse pumping lasers where both are resonant to the cavity mode exhibits a stationary state with an ordered pattern even below the self-organization threshold for sufficiently strong longitudinal pumps [10].

Experiments have shown that it is possible to trap and cool an atom inside a cavity [11], even if the cavity field consists only of one photon [12, 13].

Addressing of the particle's motion works best for quantum emitters with sharp transitions such as ions or atoms but manipulation via the effective polarization is also possible in the case of molecules in standing wave [14] or ring cavities [15], or macroscopic particles such as levitated dielectric micron-sized spheres [16–18]. By the technique of feedback control, where the depth of the optical potential is modified depending on the real-time observed atomic position the storage time of the atom can be increased and the temperature decreased in orders of magnitudes [19, 20].

Typically, the driving is done either by direct pumping into the cavity mode via one of the side mirrors (longitudinal pumping), or indirectly via light scattering of the atom into the field mode (transverse pumping). In such a case, in a properly chosen rotating frame the effective combined optical potential can be rendered time independent and the analysis greatly simplifies.

Here we depart from this scenario to consider frequency beatings between the two pumps.

While dynamics in the regime where each pump acts alone is well understood, extra forces arise from the interference between photons of different frequencies: i) scattered from the transverse light field and ii) entering the cavity mode from the longitudinal pump. The immediate effect of this interference force is to generate a time-dependent optical potential with a time modulation leading to a sign change that effectively induces the particle into undergoing jumps along the cavity sites in a quasi-random walk fashion. We analyze such a regime both numerically and via simplified analytical models. The mechanism is similar to the ones exploited in the creation of artificial potentials in optical lattices [21]. By discretization of the trajectories, we analyze the emerging discrete process via its correlation function and find that it corresponds to an environment with a very short memory. The goal of this analysis is to provide a quantum optical setting in which the classical random walk can be observed and which would constitute a starting point into further generalizations into the quantum regime. This is similar to previous works on implementation of the quantum random walk with photons [22], atoms in optical lattices [23] and ions in traps [24]. Our analysis is mainly based on a single two-level system but we discuss as well an extension involving doped micro-spheres where the field addresses a collective atomic variable (along the lines of hybrid optomechanics with doped mechanical resonators [25]).

The master thesis is organized as follows: in Chapter 2 we explain the setup and the mathematical description of the semi-classical system until we derive the equations of motion for operator expectation values. The resulting dimensionless system of coupled differential equations is solved numerically in Chapter 3, where we try to emphasize the build up of the particle motion with random walk character for strong enough transverse driving. Chapter 4 gives a brief introduction into the one dimensional random walk and the Langevin theory of Brownian motion. In chapter 5 we derive analytical expressions of the forces that act on the particle in a steady state of the cavity field amplitude and the atomic polarization. We also show the coincidence of this derivation with a simplified model, where we neglect the back-action of the atomic position on the cavity field and the polarization for weak atom-light coupling. The numerical results are presented in Chapter 6 where the random nature of the system is analyzed statistically and compared to the results that we would expect for a classical random walk on a line and for linear diffusion processes. Chapter 7 deals with possible variations of the setup and the resulting modifications in the equations of motion. We discuss the cases of a saturated atom, of a doped-nanosphere instead of a single atom and of transverse frequency comb driving. We summarize the results and come to a conclusion in Chapter 8. A short outlook on future perspectives for further investigations of the system is presented and we briefly discuss the implementation of our model and the possibility of implementing a quantum random walk.

# Chapter 2

# Cavity QED with moving atoms

## 2.1 Optical cavities and quantized electromagnetic field

An optical resonator consists of two mirrors that reflect electromagnetic waves. The condition for the electric field to be zero at the boundaries of the reflecting mirrors, separated from each other with distance $L$, leads to quantized cavity modes in each spatial direction, characterized by the wave numbers $k_i = \frac{2\pi n_i}{L}$ and frequencies $\omega_i = ck_i$, where $i \in \{1, 2, 3\}$ is the spatial direction and $n_i \in \mathbb{Z}_0$. To each wave vector belongs a mode function $\vec{u}_{\vec{k}}(\vec{x}, t)$ that determines the shape of the cavity mode. In general the mode functions form a complete orthonormal set. The separation between two resonance frequencies is the free spectral range $\omega_{FSR} = \frac{c\pi}{2L}$. The cavity mirrors have a finite transparency so photons will leak out through the mirrors and get lost in the environment. The electromagnetic field intensity inside the resonator will decay in time because of these losses. The rate of photon decay is $\kappa$. It is also the inverse lifetime of a photon inside the cavity. An important quantity to characterize a cavity is the optical finesse $\mathcal{F} = \frac{\omega_{FSR}}{\kappa}$. It gives the mean number of round trips of a photon before it leaves the cavity and thus it is also a value for the amplification of the input field.
We want to consider a single mode cavity along the longitudinal axis , which we declare as the x-axis. The wave vector is $\vec{k} = k_c\vec{e}_x$ and the resonance frequency is $\omega_c$. We model the mode function as $\vec{u}_{k_c}(x) = \sqrt{\frac{2}{L}}\vec{e}_{(\lambda)}\cos(k_c x)$, where $\vec{e}_{(\lambda)}$ is a unit vector describing the polarization in the plane perpendicular to the wave vector. With these definitions the mode function is normalized to one. The quantized vector potential operator of the electromagnetic field is

$$\vec{A}(x,t) = \sqrt{\frac{\hbar}{2\omega_c\epsilon_0}}\vec{u}_{k_c}(x)(ae^{i\omega_c t} + a^\dagger e^{-i\omega_c t}). \tag{2.1}$$

In analogy to the quantum mechanical harmonic oscillator $a^\dagger$ and $a$ are the bosonic creation- and annihilation operators of the cavity field acting on the Fock-Space $\{|n\rangle\} = \mathcal{H}_c$ of photon number states with commutator $[a, a^\dagger] = 1$. In absence of a scalar field we get the electric and magnetic field over the identities

$$\vec{E}(x,t) = -\frac{\partial\vec{A}(x,t)}{\partial t} \qquad\qquad \vec{B}(x,t) = \nabla \times \vec{A}(x,t). \tag{2.2}$$

The Hamiltonian of the electromagnetic field inside the cavity in the Coulomb gauge $\nabla \cdot \vec{A} = 0$ and without the zero point energy is

$$H = \frac{1}{2}\int dx(\epsilon_0|\vec{E}|^2 + \mu_0^{-1}|\vec{B}|^2) \tag{2.3}$$

$$= \hbar\omega_c a^\dagger a. \tag{2.4}$$

If the cavity is driven resonantly by a laser from the left side along the x-direction the output field on the right side of the cavity samples a coherent state, which can be described by the displacement operator $D(\alpha) = e^{\alpha a^\dagger - \alpha^* a}$ acting on the vacuum field:

$$|\alpha\rangle = D(\alpha)|0\rangle = e^{-|\alpha|^2}\sum_{n=0}^{\infty}\frac{(\alpha)^n}{\sqrt{n!}}|n\rangle. \tag{2.5}$$

The time evolution of the operator $H_{p,c} = i\eta_L(a^\dagger - a)$ exactly gives a displacement with a real factor increasing linearly in time:

$$e^{-iH_{p,c}t} = D(\eta_L t). \tag{2.6}$$

If the driving laser is not resonant with the cavity mode we have to consider the rotation of the operator in the pump term in time. The Hamiltonian for a cavity driven with a laser of pumping rate $\eta_T$ and frequency $\omega_L$ is

$$H = \hbar\omega_c a^\dagger a + i\eta_L(a^\dagger e^{-i\omega_L t} - a e^{i\omega_L t}). \tag{2.7}$$

## 2.2 Atom-light interaction

The simplest model for an atom is that of a qubit with two relevant energy levels, the ground and the excited states. To test the interaction of both internal and motional degrees of freedom with light, atoms are passed through optical cavities. A typical procedure is illustrated in Fig. 2.1, where atoms are launched from an atomic fountain. The flux has to be very low to be sure that there is only one atom traversing the resonator space at any time. The atom also has to be laser cooled beforehand to have larger interaction time with the cavity field. The atomic transition has to be chosen in the right energy range. For example, in Pinkse et al. (2000) [13] the parameters used are: the $5^2S_{1/2}F = 3 \leftrightarrow 5^2P_{3/2}F = 4$ transition of $^{85}$Rb atoms at a wavelength of $\lambda = 780$nm in a cavity with finesse $\sim 4.3 \times 10^5$ at length $116\mu$m.
The qubit can absorb a photon of the cavity field and go from the ground into the excited state. We define the atomic ground and excited state $|g\rangle = \begin{pmatrix}0\\1\end{pmatrix}$ and $|e\rangle = \begin{pmatrix}1\\0\end{pmatrix}$. The atomic annihilation and creation operators are defined in terms of Pauli operators

$$\sigma_x = \frac{\sigma_+ + \sigma_-}{2} \qquad\qquad \sigma_y = i\frac{\sigma_+ - \sigma_-}{2}. \tag{2.8}$$

The angular momentum commutation relation $[\sigma_a, \sigma_b] = 2i\epsilon_{abc}\sigma_c$ gives us the useful commu-

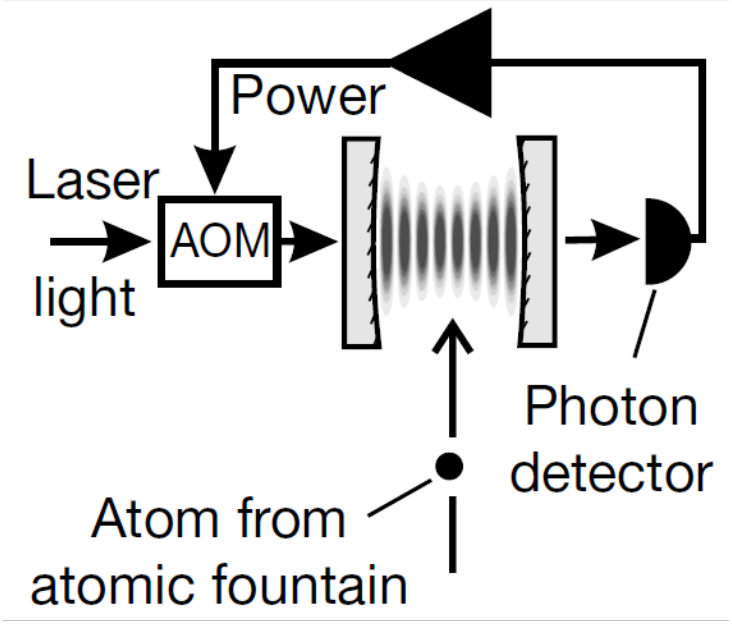


Figure 2.1: Typical experimental setup for cavity QED with atoms and longitudinal driving from [13]. Atoms are launched by a low flux fountain into the cavity from transverse direction. An AOM (acousto-optic modulator) increases the light intensity. Output photons are detected on the right side.

tators

$$[\sigma_\pm, \sigma_z] = \mp 2\sigma_\pm. \tag{2.9}$$

In the classical picture, the atom has a dipole moment due to the electron cloud surrounding the atomic nucleus. An external electric field induces charge separation and polarizes the atom. We consider the interaction in the dipole approximation, where the atomic diameter is much smaller than the wavelength of the electric field so the internal structure of the atom and the electron wave function do not play a role. The energy of a dipole in an electric field is given by $H_{int} = -\vec{d}\vec{E}$.
The dipole operator is

$$\vec{d} = \vec{\mu}_{ge}(\sigma_+ e^{-i\omega_a t} + \sigma_- e^{i\omega_a t}) \tag{2.10}$$

where the transition operators rotate in time with the atomic transition frequency $\omega_a$. They can be written as tensor products of the atomic states to visualize their meaning as transition processes, i.e. $\sigma_+ = |e\rangle\langle g|$ and $\sigma_- = |g\rangle\langle e|$. The dipole matrix element $\vec{\mu}_{ge} = \langle g|e\vec{r}|e\rangle$ is real since it must have the same amplitude for the creation and the annihilation of the atomic transition. It can be calculated by inserting the electron wave functions of the specific atomic orbital.
We assume the cavity mode frequency and the atomic transition frequency to be close to each other, so the rotating wave approximation can be applied, which is neglecting the fast oscillating

and non-energy conserving terms in $H_{int}$ and get

$$H_{int} = i\sqrt{\frac{\hbar\omega_c}{2\epsilon_0}}\vec{\mu}_{ge} \cdot \vec{u}_{k_c}(x)(\sigma_+ a - \sigma_- a^\dagger) \tag{2.11}$$

$$= i\hbar g(x)(\sigma_+ a - \sigma_- a^\dagger). \tag{2.12}$$

We defined the coupling function $g(x) = g_0 \cos(k_c x)$ with amplitude $g_0 = \sqrt{\frac{\hbar\omega_c}{\epsilon_0 L}}\vec{\mu}_{ge}\vec{e}_{(\lambda)}$. It depends explicitly on the atomic position and is maximal when dipole moment and polarization vector are parallel.
The total Hamiltonian $H = H_0 + H_{int}$ consisting of the cavity field energy, the atomic energy and dipole interaction is known as the Jaynes-Cummings model

$$H_{JC} = \hbar\omega_c a^\dagger a + \frac{\hbar\omega_a}{2}\sigma_z + i\hbar g(x)(\sigma_+ a - a^\dagger \sigma_-) \tag{2.13}$$

which is the simplest form of atom-field interaction. The eigenstates of this Hamiltonian are linear combinations of the atom-field product states and are called dressed-states

$$|\pm\rangle = \frac{1}{\sqrt{2}}(|n, e\rangle \pm |n+1, g\rangle). \tag{2.14}$$

The eigenvalues of the interaction term are $\pm\hbar\Omega$, where the Rabi-frequency is

$$\Omega = g(x)\sqrt{n+1}. \tag{2.15}$$

## 2.3 Cavity cooling

In a system of an atom trapped inside an optical cavity with the ability to move along the x-direction and a laser pumping the cavity parallel to the axis the effect of cavity cooling can be seen. The system can be described by the Hamiltonian

$$H = \hbar\omega_c a^\dagger a + \frac{\hbar\omega_a}{2}\sigma_z + i\hbar g(x)(\sigma_+ a - a^\dagger \sigma_-) + i\eta_L(a^\dagger e^{-i\omega_L t} - a e^{i\omega_L t}). \tag{2.16}$$

Depending on the detunings between the pump laser and the mode and between pump laser and atomic transition the particle's momentum can be reduced until it gets trapped inside a potential well. This can be understood by the dispersive effect of the atom onto the electromagnetic field. The particle inside the cavity is a dispersive medium, that changes the refractive index. A red-detuned pump laser ($\Delta_a < 0$) shifts the cavity detuning $\Delta_C$ the way that it is more in resonance when the particle stays in positions of high field intensity. The rearrangement of the cavity fields shape according to the particles position, happens with a time delay, because the cavity can not react instantaneously. This leads to the phenomenon that the particle always has to climb a potential hill when it tries to moves towards the actual minimum, so it feels a friction force. Another explanation refers to the scattering process of photons and the atom. If a pump laser photon scatters off the atom it needs to have the energy of the cavity mode to fit into the resonator. If the pump is red detuned, the photons take the lack of energy by a momentum transfer with the atom. The atom gives kinetic energy to the photon, so that it has the frequency of

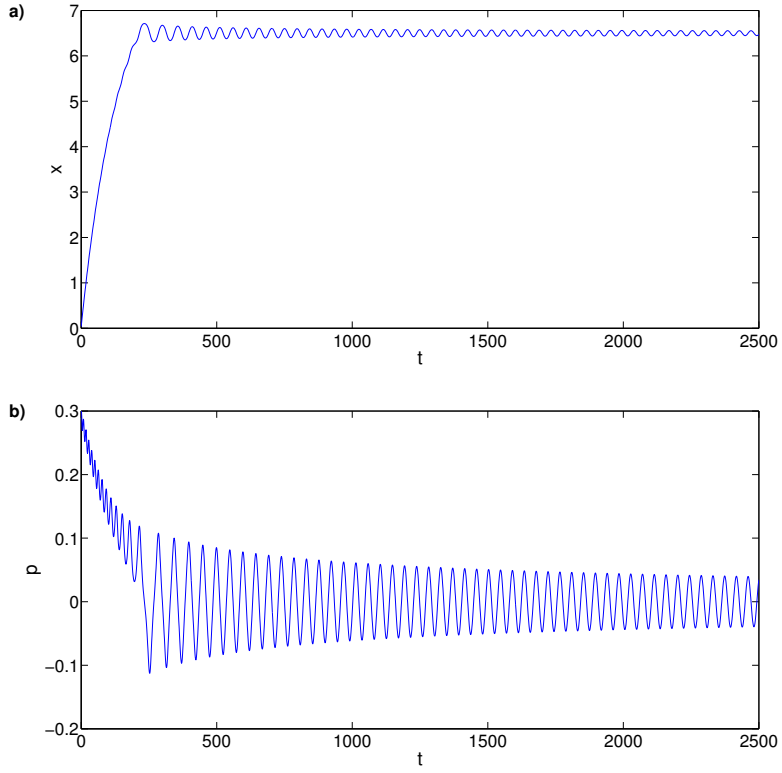


Figure 2.2: Cooling of the atomic motion. a)The particle is attracted to positions of high field intensity. It feels a friction force [6] while moving through the cavity until it is trapped inside a potential well, where it oscillates back and forth. b)The initially positive momentum decreases until it oscillates around zero.

the mode. Since kinetic energy is taken from the atom it slows down, thus gets cooled. On the other hand a blue detuned pump laser would heat up the atomic motion in a similar way. The atomic motion might be quantized in phonon excitations. The scattering processes can result in the absorption of a phonon by the impinging photon or in the absorption of a photon and creation of phonons.
There is a quantum mechanical limit to cavity cooling based on Heisenberg's uncertainty principle. The photons have an energy uncertainty of $\Delta E = \frac{\hbar}{\Delta t}$ according to their mean life time, which is the inverse decay rate $\Delta t^{-1} = \kappa$. That means the atom can transfer its kinetic energy to the photon field up to the minimum of $\hbar\kappa$.
Laser cooling in free space is based on the isotropic spontaneous photon emission of an atom so that the recoil momentum is zero in time average and the deceleration of atomic motion in a specific direction is accessible by shooting near resonant laser light on the atom. However the cavity cooling effect is independent of spontaneous emission and works in general with any polarizable particle. That conclusion lead to the manipulation of motion of the broad variety of objects mentioned in the introduction. It is also used to cool the quantized motion of mechanical oscillators inside cavities like e.g. suspended mirrors, membranes [29–31] or dielectric sub-micron particles [16–18] in the field of cavity-optomechanics.
For strong light-matter coupling cooling can be explained physically by a Sisyphus-type mech-

anism. The eigenenergies of the dressed atom-light states modulate spatially with the cavity mode function. If the system is in the ground state, it is more probable that it gets excited into the energetically lower dressed state at minima of the spatial modulation of the eigenenergies. Otherwise the maxima of the eigenstate are in resonance with the cavity, where the emission of photons is likely. By this scheme, the coupled system has lower energy, when the photon is absorbed and after climbing up the potential hill the photon is lost by emission and the system is back in the ground state.

## 2.4 Doubly pumped cavity

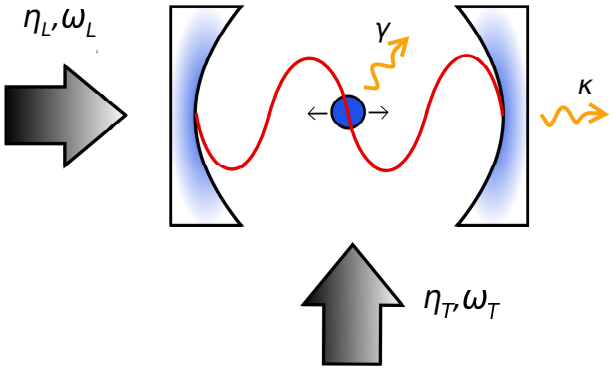


Figure 2.3: Scheme of a double pumped cavity. An atom is trapped inside a cavity of two highly reflecting mirrors with a standing wave mode function (red line). The longitudinal pump laser has a photon pump rate $\eta_L$ with frequency $\omega_L$. The transverse laser with pump strength $\eta_T$ and frequency $\omega_T$ is slightly detuned to the longitudinal one. The atom decays spontaneously with rate $\gamma$ while photons leave the cavity through the right mirror with rate $\kappa$.

A transverse pump directly drives the polarization of the atom and induces additional oscillations of the dipole moment. We model this operation analog to the initial dipole moment operator but rotating with the transverse pump frequency $\omega_T$. This pump only increases the photon number of the cavity field by scattering laser beam photons off the atom and into the cavity. It does not drive the cavity field directly since the propagation of these photons is perpendicular to the cavity axis. The photon pump rate of the transverse laser beam is denoted by $\eta_T$.
The full Hamiltonian in the rest frame is

$$\begin{aligned} H =& \hbar\omega_c a^\dagger a + \frac{\hbar\omega_a}{2}\sigma_z + i\hbar g(x)(\sigma_+ a - a^\dagger \sigma_-) + i\hbar\eta_L(a^\dagger e^{-i\omega_L t} - a e^{i\omega_L t}) \\ &+ i\hbar\eta_T(\sigma_+ e^{-i\omega_T t} - \sigma_- e^{i\omega_T t}). \end{aligned} \tag{2.17}$$

We now want to change the time dependency of this operator the way that only the transverse pump term depends on time. For that we apply a unitary transformation $U = e^{i\hbar\omega_L(a^\dagger a + \frac{\sigma_z}{2})t}$ to the Hamiltonian. To get the transformed operator we also have to keep in mind the change of

the Schrödinger equation

$$
\begin{aligned}
i\partial_t|\psi\rangle &= H|\psi\rangle && (2.18)\\
|\psi'\rangle &= U|\psi\rangle && (2.19)\\
i\partial_t|\psi'\rangle &= i((\partial_t U)|\psi\rangle + U\partial_t)|\psi\rangle && (2.20)\\
&= (-\hbar\omega_L(a^\dagger a + \sigma_+\sigma_-) + UHU^{-1})|\psi'\rangle. && (2.21)
\end{aligned}
$$

In the frame rotating with $\omega_L$ the Hamiltonian is

$$
\begin{aligned}
H = &-\hbar\Delta_c a^\dagger a - \frac{\hbar\Delta_a}{2}\sigma_z + i\hbar g(x)(\sigma_+ a - a^\dagger\sigma_-) + i\hbar\eta_L(a^\dagger - a)\\
&+ i\hbar\eta_T(\sigma_+ e^{i\Delta_T t} - \sigma_- e^{-i\Delta_T t})
\end{aligned}
\tag{2.22}
$$

with detunigs $\Delta_\nu = \omega_L - \omega_\nu$ and $\nu \in \{c, a, T\}$. Notice that the time dependency cannot be eliminated. This is an for now unexplored regime.

## 2.5 Master equation approach

The system is coupled dissipatively to the vacuum modes of the electromagnetic field. Coupling to thermal modes can be neglected in the optical domain [26]. We consider the damping of the cavity field by losses through the mirrors into the environment. The rate of photons that leak out of the cavity is $\kappa$. The atomic state is damped by spontaneous emission characterized by the emission rate $\gamma$. From now on we set $\hbar \equiv 1$. The evolution of the density matrix that describes the quantum state of the product space of the cavity field and the two level atom is given by the master equation

$$\dot{\rho} = -i[H,\rho] + \mathcal{L}_{cav}\rho + \mathcal{L}_{atom}\rho. \tag{2.23}$$

In addition to the Von Neumann equation for the density matrix, the dissipative processes lead to Liouville operators in Born-Markov approximation

$$
\begin{aligned}
\mathcal{L}_{cav}\rho &= \kappa(2a\rho a^\dagger - a^\dagger a\rho - \rho a^\dagger a) && (2.24)\\
\mathcal{L}_{atom}\rho &= \gamma(2\sigma_-\rho\sigma_+ - \sigma_+\sigma_-\rho - \rho\sigma_+\sigma_-). && (2.25)
\end{aligned}
$$

Since the atomic position will be treated classically in further proceedings we neglected the recoil momentum on the atom from the spontaneously emitted photons.
The master equation allows us to calculate the expectation value and the time derivative for any system operator $A$ by $\langle A\rangle = \mathrm{Tr}[\rho A]$ and $\langle \dot{A}\rangle = \mathrm{Tr}[\dot{\rho} A]$. The second equation refers to the physical equivalence of the Heisenberg- and Schrödinger- picture, that allows to swap the time derivative from the operator to the density matrix.
For a given initial density matrix the master Equation can give the evolution of the full quantum model. A common strategy is to change the representation of the cavity field by the use of quasi-probability distributions, which leads to stochastic c-number differential equations of Fokker-Plank-Equation type [27].

## 2.6 Quantum Langevin approach

An equivalent alternative to the master equation is to look at the evolution of the operators by calculating the quantum Langevin equations. In principle we calculate the Heisenberg equations for $a$ and $\sigma_-$ and add a damping term and a noise operator, that arises from the coupling to vacuum fluctuations [28]. With (2.22) this gives

$$\dot{a} = i[H, a] - \kappa a + F_1 \tag{2.26}$$
$$= (-\kappa + i\Delta_c)a - g(x)\sigma_- + \eta_L + F_1 \tag{2.27}$$
$$\dot{\sigma}_- = i[H, \sigma_-] - \gamma\sigma_- + F_2 \tag{2.28}$$
$$= (-\gamma + i\Delta_a)\sigma_- - g(x)a\sigma_z - \eta_T\sigma_z e^{i\Delta_T t} + F_2 \tag{2.29}$$

We see that $a$ oscillates with $\Delta_c$, decays by $\kappa$, is driven by $\eta_L$, feels a back action depending on the atomic polarization and the atomic position and feels fluctuations coming from the noise term $F_1$. The equation for $\sigma_z$ is similar except that the sign of the driving, the back action and the noise depends on the atomic state and the driving remains time dependent due to the detuning between the two lasers.
The noise operators $F_{1/2}$ have mean zero and their two time correlation functions are delta-correlated

$$\langle F_i \rangle = 0 \qquad\qquad \langle F_i(t)F_i(t')\rangle \propto \delta(t - t'). \tag{2.30}$$

They apply random forces on the atom and the cavity but since we will proceed with the expectation values of $a$ and $\sigma_z$ it is not necessary to specify the noise operators here.

# Chapter 3

# Simulation of a quasi-random walk

## 3.1 Classical limit with a weakly-driven atom

In the semi-classical limit position and momentum of the atom are treated as classic variables while the cavity field and the atomic states are treated as operators. This holds especially for atoms that have a temperature above the recoil temperature, i.e. $k_B T \gg \hbar\omega_r$ [26]. The recoil frequency times Planck constant is the energy transfer, that the atom experiences by a collision with a photon of the cavity field, defined by $\hbar\omega_r = \frac{\hbar^2 k^2}{2m}$. We assume Newtonian equations of motion for $x$ and $p$ and take the expectation values of eq. (2.27) and (2.29). We also suggest low saturation of the atom. If the pump laser is far detuned from the atomic transition, the excited state will be hardly occupied. So it is reasonable to set $\sigma_z = -\mathbb{1}$. Also weak pumping is necessary to fulfill this. (2.27) and (2.29) become linear in the sense that there are no operator products any more. We denote $\langle a \rangle = \alpha$ and $\langle \sigma_- \rangle = \beta$. Quantum correlations of the atom and the cavity field are neglected so that the expectation values separate, i.e. $\left\langle \sigma_+ a - a^\dagger \sigma_- \right\rangle = 2iIm\{\beta^* \alpha\}$. By these assumptions we reduce our setup to a totally classical system. We further transform to the dimensionless variables

$$t \to t = t\kappa \tag{3.1}$$

$$x \to x = kx \tag{3.2}$$

$$p \to p = \frac{p}{k} \tag{3.3}$$

Also the time derivatives have to be taken with respect to $t\kappa$. The dimensionless system is given by the four coupled differential equations

$$\dot{x} = 2\omega_r p \tag{3.4}$$

$$\dot{p} = g'(x) 2Im\{\beta^* \alpha\} \tag{3.5}$$

$$\dot{\alpha} = (-\kappa + i\Delta_c)\alpha - g(x)\beta + \eta_L \tag{3.6}$$

$$\dot{\beta} = (-\gamma + i\Delta_a)\beta + g(x)\alpha + \eta_T e^{i\Delta_T t} \tag{3.7}$$

All cavity parameters are now divided by $\kappa$.
(3.4)- (3.7) is the system of equations of motion we will analyze in further chapters. It is important to point out the pure classical nature of these equations. By taking the expectation values and neglecting noise we lost any quantum feature and deal with a not fluctuating electric field and an atom that is reduced to a one dimensional oscillating dipole.

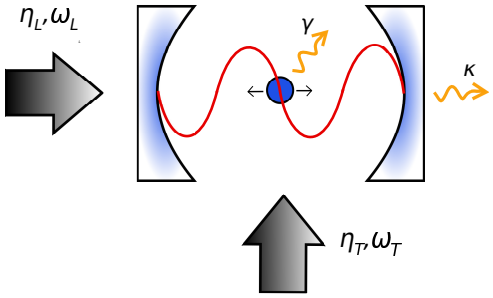


Figure 3.1: Schematic setup which is described by the set of differential equations Eq. (3.4)-(3.7) and which we solve numerically.

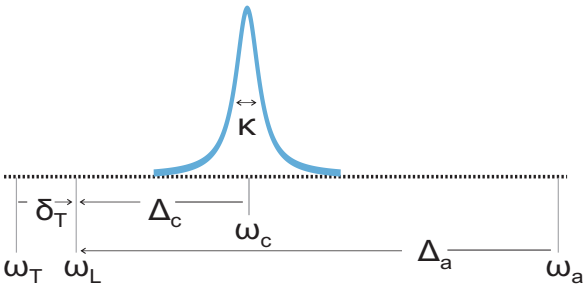


Figure 3.2: Illustration of the frequencies and detunings as defined in the equations of motion and used in the numerics. The detunings are taken with respect to the longitudinal driving frequency such that $\Delta_c < 0$ corresponding to the stable regime of cavity QED with moving atoms and $\Delta_a < 0$ that corresponds to $U_0 = g^2/\Delta_a < 0$ as for high-field seekers.

## 3.2 Trajectories and potentials

We now solve our system of couple differential equations numerically. The single longitudinal driving case showed cooling of the particles motion until it is trapped inside a potential well. The momentum oscillates around a linear falling curve until it fulfills a damped oscillation around zero. The field intensity and the atomic occupation oscillate very fast around a constant low value. From the moment on where the particle gets trapped ($t \sim 900$ in Fig. 3.2a)) the potential (colored background in the first plot in Fig. 3.2a)) does not change its sign along the time evolution any more, although the back action of the particle on the potential still decreases the potential amplitude while moving through the local minimum positions.

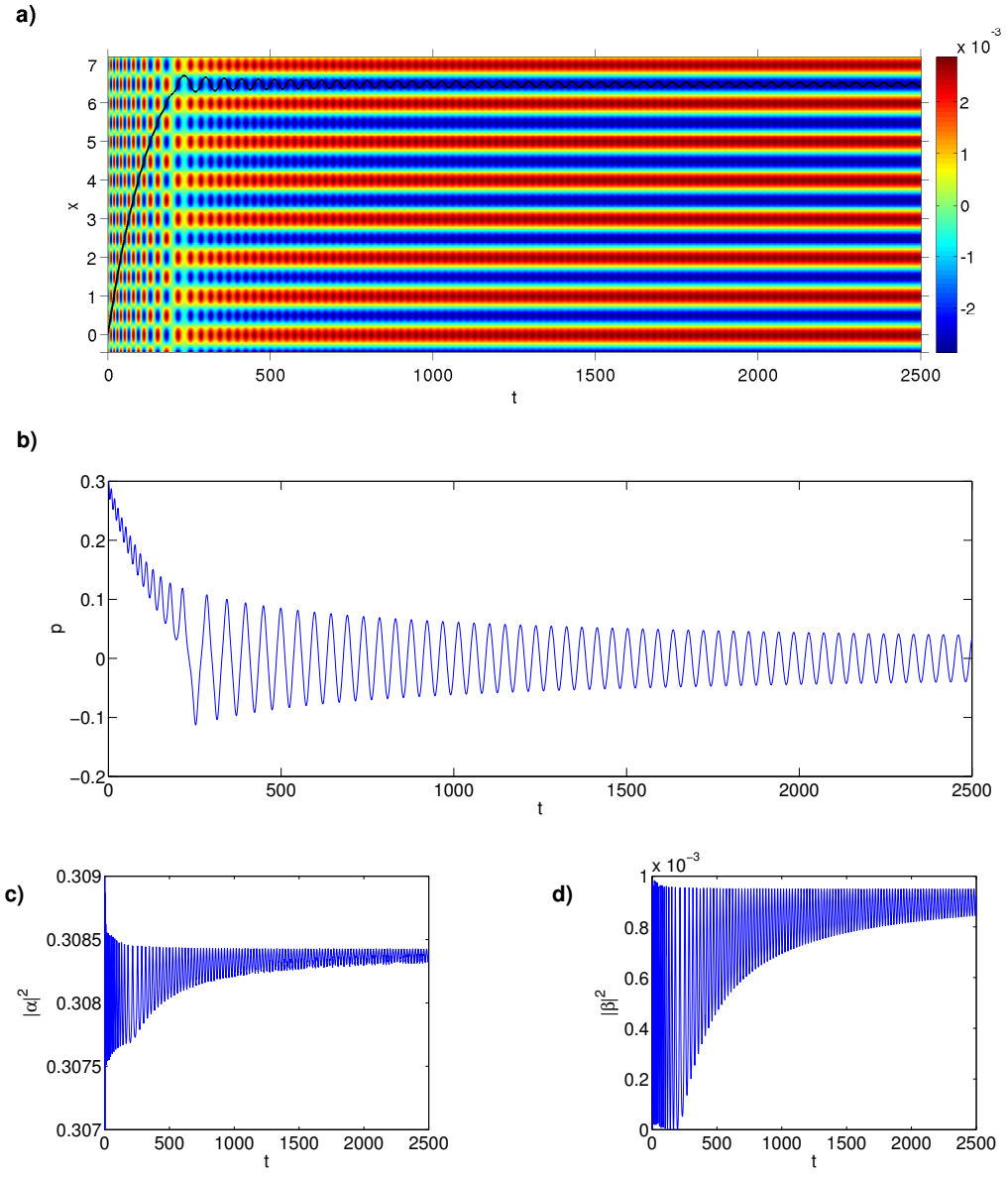


Figure 3.3: Longitudinal pumping of the cavity with a low saturated atom for parameters $\gamma = 1$, $g = 0.1$, $\Delta_a = -1.5$, $\Delta_c = -1.5$, $\Delta_T = 0.2\pi$, $\eta_L = 1$, $\omega_r = 0.1$, $k = 2\pi$ and initial values $x_0 = 3.49 \times 10^{-3}$, $p_0 = 0.3$ and $\alpha_0 = \beta_0 = 0$, with $x$ and $p$ in units of $k$ ($\hbar \equiv 1$). a) The potential $-2g(x)Im\{\beta^*\alpha\}$ is plotted as colored background of the trajectory, where the bar on the right gives the color scheme for the value of the amplitude. Notice that with $k = 2\pi$ the vertical axis is in units of the mode wavelength $\lambda_c$. b) The momentum decreases until it oscillates around zero. c) The cavity field intensity oscillates with an exponentially decaying amplitude so that it converges constant value around $0.3083$. d) The atomic occupation behaves similar to the field intensity and converges to a value around $0.9 \times 10^{-3}$.

Now we leave all other parameters as they were and just tune up the transverse pump rate $\eta_T$. We see that the particle gets trapped much earlier. The transverse pump increases the total

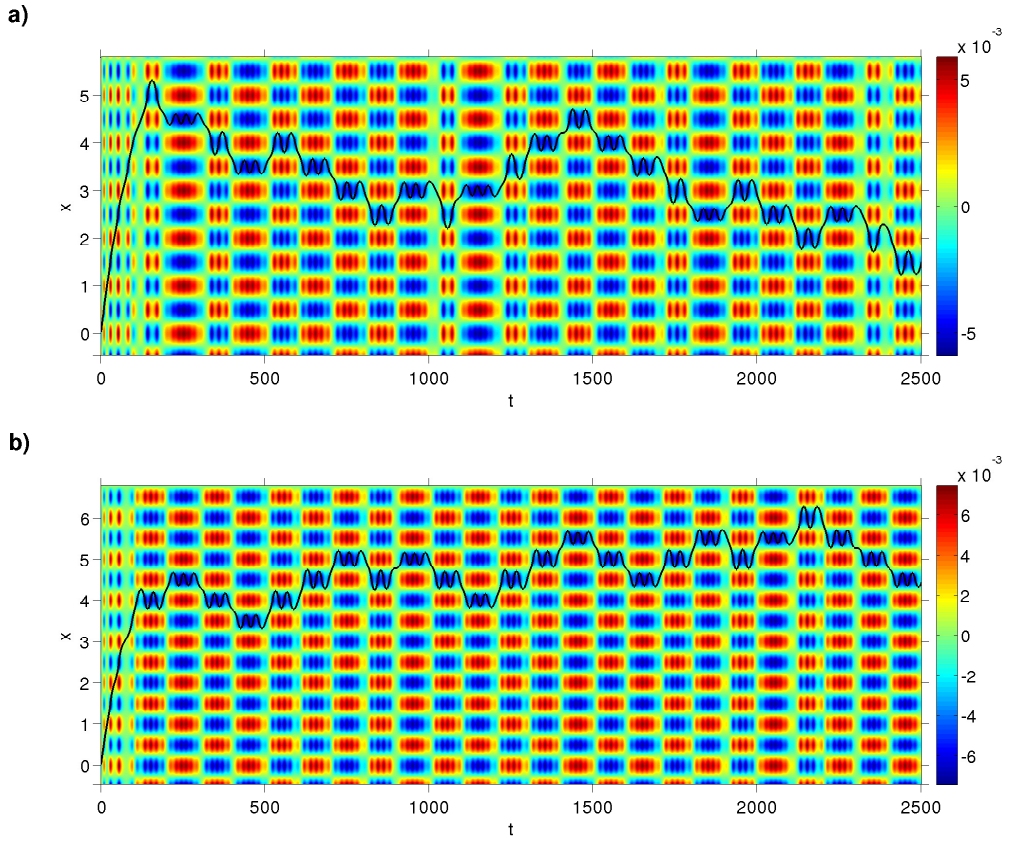


Figure 3.4: Doubly pumped particle motion. a) Trajectory for $\eta_T = 5 \times 10^{-2}$. The mean atom occupation over the time range of integration is $\langle|\beta|^2\rangle = 1.7 \times 10^{-3}$. All other cavity parameters were chosen as before in Fig. 3.3. b) Trajectory for $\eta_T = 0.1$ and mean atom occupation $\langle|\beta|^2\rangle = 3 \times 10^{-3}$.

field intensity and the cooling gets stronger. For $\eta_T = 0.1$ the motion and the potentials shape are still quiet irregular. When the transverse pump becomes larger the cooling motion is gone since the particle is trapped immediately. The potential is dominated by the oscillation in space and time of pure cosine shape. The oscillation period in time is the detuning frequency between the two driving lasers. The back action effect is reduced to small amplitude modulations above the dominant oscillation in time and is negligible for trajectories in the regime of Fig. 3.4a). The direction in which the particle jumps to the next trapping site when the potential flips sign is determined by the phase between the two coupled oscillations, i.e. the oscillation inside a potential well when the particle is trapped and the oscillation in time of the potential itself. But this seems to be hard to predict since the amplitude of the trap is not constant over one period. Additionally the initial conditions and all parameters might influence the transient.

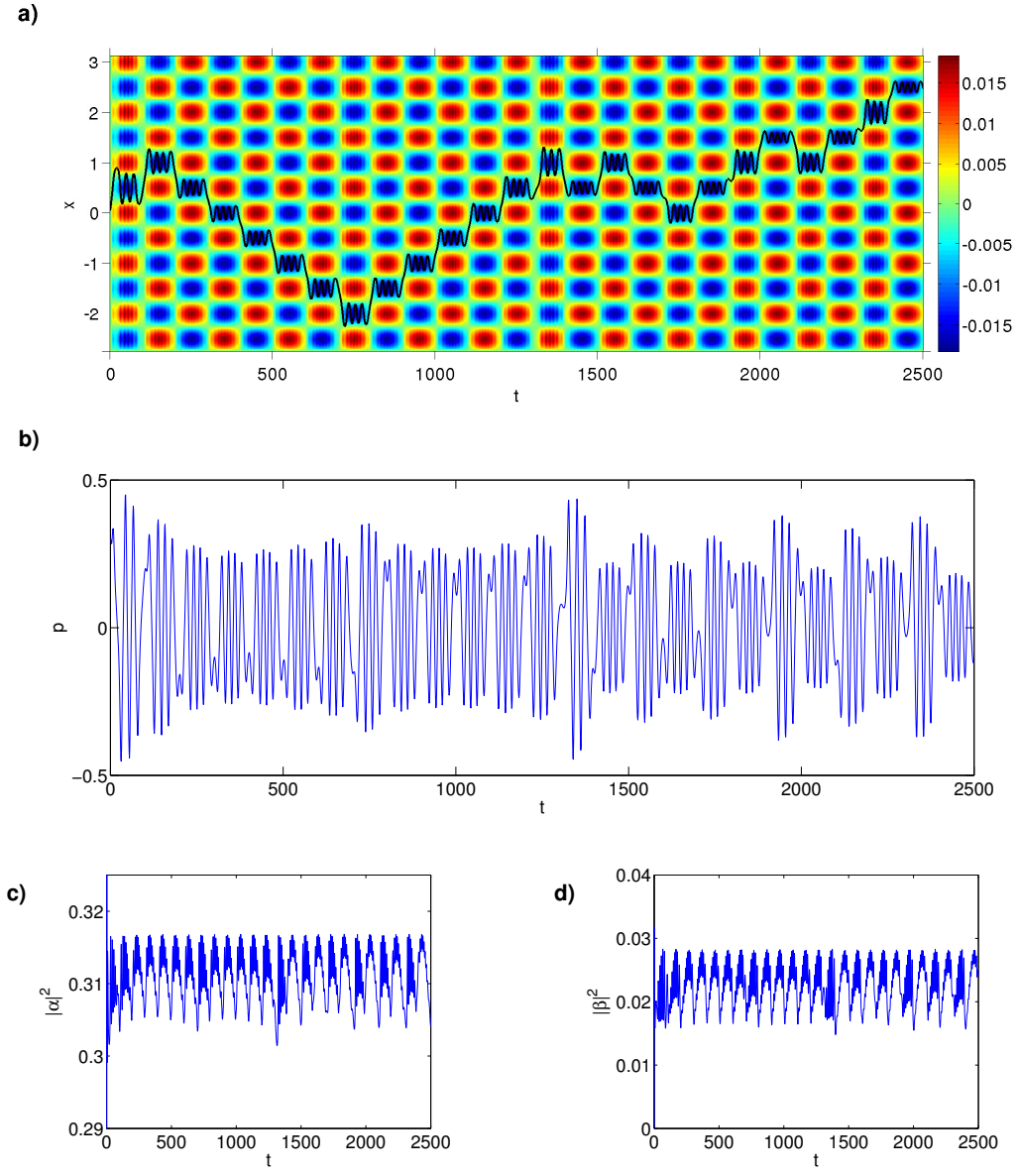


Figure 3.5: Longitudinal pumping of the cavity with transverse pump rate $\eta_T = 0.5$. a) The particle oscillates at integer positions for even and half integer position for odd numbers of jumps, which occur after time periods of $\frac{\pi}{\Delta_T} = 50$. b) The momentum starts a new oscillation around zero with modified amplitude at each time period. c) The field intensity oscillates with the shape of a squared sine function, shifted along the y-axis about a value of $0.31$. d) The atomic occupation oscillates analog to the field intensity and is shifted about a value of $0.02$.

# Chapter 4

# Basic concepts of the one dimensional random walk

## 4.1 Binomial and Gaussian distribution

The classical random walk is relevant in diverse scientific field. E.g. is the basis for many computer algorithms [32] and is even used in the context of stock market prices [33]. In physics and biology it is a useful model for the description of diffusion processes.
The random walk on a line describes the following abstract situation: a particle moves on a one dimensional equidistant lattice with discrete positions $\{x_i\}$ with $i \in \mathbb{Z}$ and lattice constant $a$. At the times steps $\{t_N = N\tau\}$, with $N \in \mathbb{N}$ and a period $\tau \in \mathbb{R}_{>0}$, the particle jumps to an adjacent position with probability $p$ for movement to the right and $q = 1 - p$ to the left. For a particle that started at the origin the distribution of jumps to the right $r$ is

$$P_N(r) = \frac{N!}{r!(N-r)!} p^r q^{N-r}. \tag{4.1}$$

The binomial distribution has mean $\langle r \rangle = Np$ and variance $\langle (\Delta r)^2 \rangle = Npq$. The arriving position is $n = r - (N - r) = 2r - N$. We substitute $n$ for $r$ in the probability distribution and get the mean arrival position $\langle n \rangle = N(p - q)$ with variance $\langle (\Delta n)^2 \rangle = 4Npq$. Referring to the central limit theorem [35] the binomial distribution becomes a Gaussian for very large $N$. The limiting distribution is

$$P_N(n) = \frac{1}{\sqrt{2\pi 4Npq}} e^{-[n-N(p-q)]^2/(8Npq)}. \tag{4.2}$$

We define $x = an$ and $t = N\tau$ and express the distribution in terms of the new variables $x$ and $t$:

$$P(x,t) = \frac{dn}{dx} P_N(n) = \frac{1}{\sqrt{2\pi \left\langle (\Delta x)^2 \right\rangle}} e^{-(x-\langle x \rangle)^2/(2\left\langle (\Delta x)^2 \right\rangle)}. \tag{4.3}$$

This is the Gaussian normal distribution. The first moment $\langle x \rangle = (p-q)\frac{a}{\tau}t$ gives a drift-velocity $v = (p - q)\frac{a}{\tau}$ for a biased random walk. The isotropic or unbiased case has zero mean and no drift. The second moment $\langle (\Delta x)^2 \rangle = 4\frac{pqa^2}{\tau}t = 2Dt$ is linear in time and the proportionality factor $D = 2\frac{pqa^2}{\tau}$ is the diffusion constant.

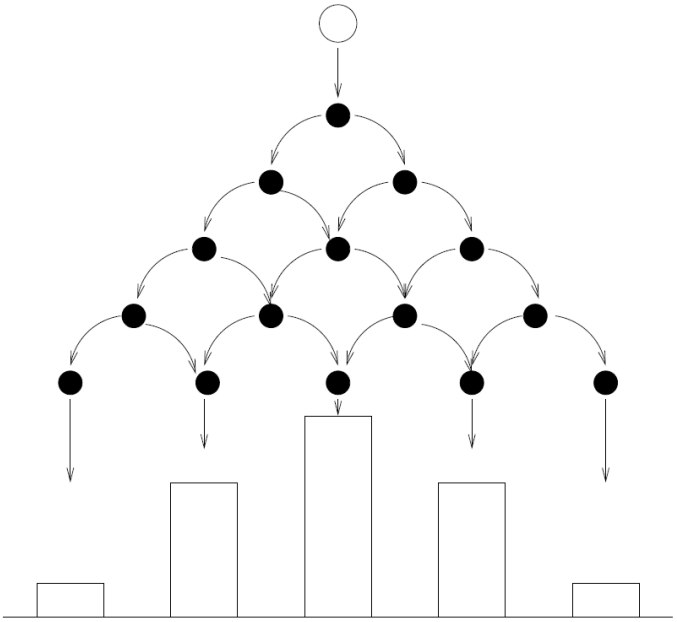

Figure 4.1: Galton's Board (Quincunx) from [44]. A board with pins arranged in a two dimensional square lattice was used by Francis Galton to demonstrate the binomial distribution. When a ball falls through the quincunx, it samples a random walk on a line with equal probabilities of moving to the left or right at the moments where it hits a pin. The spaces between the last row of pins are the bins of the final histogram.

## 4.2 Drift-diffusion equation

The random walk can also be described by the recursion relation for the probability density function

$$P(x, t+\tau) = pP(x-\delta, t) + qP(x+\delta, t) \tag{4.4}$$

It can be solved with Fourier transform techniques and the generating function [34].
Expanding $P(x,t)$ in Taylor series up to the first order in $\tau$ and second order in $\delta$ gives

$$\frac{\partial P}{\partial t} = -(p-q)\frac{\delta}{\tau}\frac{\partial P}{\partial x} + (p+q)\frac{\delta^2}{2\tau}\frac{\partial^2 P}{\partial x^2} + \mathcal{O}(\tau) + \mathcal{O}(\delta^2). \tag{4.5}$$

If the limits

$$u = \lim_{\delta,\tau\to 0}(p-q)\frac{\delta}{\tau} \qquad\qquad D = \lim_{\delta,\tau\to 0}(p+q)\frac{\delta^2}{2\tau} \tag{4.6}$$

exist and are positive, we get the drift-diffusion equation [36]

$$\frac{\partial P}{\partial t} = -u\frac{\partial P}{\partial x} + D\frac{\partial^2 P}{\partial x^2} \tag{4.7}$$

which is an example of a Fokker-Planck-equation [37]. The solution for the walker starting at position zero, i.e. initial condition $P(x,0) = \delta(x)$, is given by Eq. (4.3) with $\langle x\rangle = ut$ and $\langle \Delta x^2\rangle = 2Dt$.

## 4.3 Langevin theory of Brownian motion

We want to consider a particle that experiences a force consisting of friction and a random term. An example for a physical scenario could be a fluid particle, where the friction arises from the fluids viscosity and the random force arises from collisions with other fluid particles. Collisions happen so often that they are approximately delta correlated on the characteristic time scale of the velocity distribution of the fluid.
The equation of motion in one dimension for a particle of mass $m$ is

$$m\frac{dv}{dt} = -\gamma v + \eta(t) \tag{4.8}$$

The friction term damps the velocity by a rate $\gamma$ associated with the viscosity of the fluid. The fluctuating force $\eta(t)$ has mean $\langle \eta(t) \rangle = 0$ and two-time correlation $\langle \eta(t')\eta(t) \rangle = 2dm^2\delta(t'-t)$. We divide the equation of motion by the mass and get

$$\frac{dv}{dt} = -\lambda v + \xi(t) \tag{4.9}$$

with $\lambda = \frac{\gamma}{m}$ and $\xi = \frac{\eta}{m}$. This is a Langevin equation equivalent to (4.7) for a velocity distribution function.
We want to show that for certain conditions this case leads to a Gaussian distribution in velocity and position. First we integrate (4.9) formally to obtain the velocity:

$$v(t) = v_0 e^{-\lambda t} + \int_0^t dt' e^{-\lambda(t-t')}\xi(t') \tag{4.10}$$

The mean is

$$\langle v \rangle = v_0 e^{-\lambda t} \tag{4.11}$$

and the variance

$$\left\langle (v - \langle v \rangle)^2 \right\rangle = \left\langle (\int_0^t dt' e^{-\lambda(t-t')}\xi(t'))^2 \right\rangle \tag{4.12}$$

$$= \int_0^t \int_0^t dt' dt'' e^{-\lambda(t-t')} e^{-\lambda(t-t'')} \underbrace{\langle \xi(t')\xi(t'') \rangle}_{2d\delta(t'-t'')} \tag{4.13}$$

$$= 2d \int_0^t dt' e^{-2\lambda(t-t')} \tag{4.14}$$

$$= \frac{d}{\lambda}(1 - e^{-2\lambda t}). \tag{4.15}$$

We now want to expand the variance for small and large times. For $\lambda t \ll 1$ we expand the exponential $e^{-2\lambda t} \simeq 1 - 2\lambda t + \mathcal{O}((\lambda t)^2)$ and get the linear diffusion in velocity, for $\lambda t \gg 1$ the exponential goes to zero and the variance converges to a constant:

$$\left\langle (\Delta v)^2 \right\rangle \xrightarrow{\lambda t \ll 1} 2dt \tag{4.16}$$

$$\left\langle (\Delta v)^2 \right\rangle \xrightarrow{\lambda t \gg 1} \frac{d}{\lambda}. \tag{4.17}$$

As is a sum of Gaussian distributed random variables, namely the stochastic forces at different times, the velocity is also a Gaussian distributed random variable for small times [35], but the velocity diffusion feels losses by friction and becomes stationary distributed for large times. The position is obtained by integrating the velocity over time

$$x(t) = x_0 + \int_0^t dt' v(t'). \tag{4.18}$$

The mean position is the integrated mean velocity

$$\langle x \rangle = x_0 + \int_0^t v_0 e^{-\lambda t} \tag{4.19}$$

$$= x_0 + \frac{v_0}{\lambda}(1 - e^{-\lambda t}). \tag{4.20}$$

We define

$$X(t) = x(t) - \langle x \rangle = \int_0^t dt' e^{-\lambda t'} \int_0^{t'} dt'' e^{\lambda t''} \xi(t'') \tag{4.21}$$

and perform an integration by parts with the definitions

$$V = -\frac{1}{\lambda} e^{-\lambda t'} \qquad \frac{dV}{dt'} = e^{-\lambda t'} \tag{4.22}$$

$$U = \int_0^{t'} dt'' e^{\lambda t''} \xi(t'') \qquad \frac{dU}{dt'} = e^{\lambda t'} \xi(t') \tag{4.23}$$

leading to

$$X(t) = \int_0^t dV(t') U(t') \tag{4.24}$$

$$= [U(t')V(t')]_0^t - \int_0^t V(t') dU \tag{4.25}$$

$$= -\frac{1}{\lambda}\left(\int_0^t dt' e^{\lambda(t'-t)} \xi(t') - \int_0^t dt' \xi(t')\right) \tag{4.26}$$

$$= \int_0^t dt' \phi(t') \xi(t') \tag{4.27}$$

with $\phi(t') = \frac{1}{\lambda}(1 - e^{\lambda(t'-t)})$. Now the variance in position is

$$\left\langle (x - \langle x \rangle)^2 \right\rangle = \left\langle (X(t))^2 \right\rangle = \int_0^t \int_0^t dt' dt'' \phi(t') \phi(t'') \underbrace{\langle \xi(t') \xi(t'') \rangle}_{2d\delta(t'-t'')} \tag{4.28}$$

$$= 2d \int_0^t dt' \phi^2(t') \tag{4.29}$$

$$= 2\frac{d}{\lambda^2} \int_0^t dt' (1 - e^{\lambda(t'-t)})^2 \tag{4.30}$$

$$= \frac{2d}{\lambda^2}\left(t - \frac{2}{\lambda}(1 - e^{-\lambda t}) + \frac{1}{2\lambda}(1 - e^{-2\lambda t})\right) \tag{4.31}$$

Again we are interested in the behavior of the variance for small and large times. For $\lambda t \ll 1$ we expand the exponential functions up to the first order in $\lambda t$ and see that the dependencies on $t$ cancel each other out while for $\lambda t \gg 1$ the variance becomes linear in $t$:

$$\left\langle (x - \langle x \rangle)^2 \right\rangle \xrightarrow{\lambda t \ll 1} 0 + \mathcal{O}((\lambda t)^2) \tag{4.32}$$

$$\left\langle (x - \langle x \rangle)^2 \right\rangle \xrightarrow{\lambda t \gg 1} 2\frac{d}{\lambda^2}(t - \frac{3}{2\lambda}). \tag{4.33}$$

The particle undergoes a random walk where the slope of the variance divided by two is the diffusion constant $D = \frac{d}{\lambda^2}$. The vertical shift of the linear function can be neglected for large $\lambda$.

# Chapter 5

# Analytical results

## 5.1 Dispersive limit

In a high finesse cavity, the peaks in the transmitted light around the cavity modes are very sharp. The linewidth of the transmittance is the mirror loss rate $\kappa$. A very good cavity that has a very sharp monochromatic light signal output also has a very weakly damped electromagnetic field inside.
We want to consider the case where the atomic degrees of freedom can be eliminated adiabatically and can be expressed in terms of the cavity field operators. This holds for large atomic detunings with respect to the transverse driving frequency and the atom light coupling. Also for very high oscillation frequencies of the atom this procedure can be applied. The equations of motion for $\alpha$ and $\beta$ in low saturation limit are

$$\dot{\alpha} = (-\kappa + i\Delta_c)\alpha - g(x)\beta + \eta_L \tag{5.1}$$

$$\dot{\beta} = (-\gamma + i\Delta_a)\beta + g(x)\alpha + \eta_T e^{i\Delta_T t}. \tag{5.2}$$

For $\Delta_a \gg \{g(x), \eta_T\}$ we get

$$\dot{\beta} \simeq 0 \Rightarrow \beta \simeq \frac{g(x)\alpha + \eta_T e^{i\Delta_T t}}{\gamma - i\Delta_a} \tag{5.3}$$

and

$$-g(x)\beta \simeq \frac{-g^2(x)\alpha - g(x)\eta_T e^{i\Delta_T t}}{\gamma - i\Delta_a} \tag{5.4}$$

$$= -\frac{\gamma + i\Delta_a}{\gamma^2 + \Delta_a^2}(g^2(x)\alpha + g(x)\eta_T e^{i\Delta_T t}). \tag{5.5}$$

This leads to an effective dissipative and dispersive shift of the cavity field and an effective driving term. It is useful to write the effective transverse pump as a complex number in polar coordinates:

$$\gamma + i\Delta_a = \sqrt{\gamma^2 + \Delta_a^2} e^{i\phi} \tag{5.6}$$

with $\tan\phi = \frac{\Delta_a}{\gamma}$. Further with $c_1 = \sqrt{\gamma^2 + \Delta_a^2}$ we have $\gamma = c_1 \cos\phi$ and $\Delta_a = c_1 \sin\phi$.
The effective transverse pump becomes

$$\tilde{\eta}_T(x,t) = -\frac{g(x)\eta_T}{\sqrt{\gamma^2 + \Delta_a^2}} e^{i(\Delta_T t + \phi)}. \tag{5.7}$$

We insert Eq. (5.5) into Eq. (5.1) and get

$$\dot{\alpha} \simeq (-\kappa - \gamma(x) + i(\Delta_c - U(x)))\alpha + \eta_L + \tilde{\eta}_T(x,t). \tag{5.8}$$

We define the effective dissipative and dispersive shift of the cavity field

$$\gamma(x) = \frac{g_0^2 \gamma}{\gamma^2 + \Delta_a^2} \cos^2(k_c x) = \Gamma_0 \cos^2(k_c x) \propto \chi'' \tag{5.9}$$

$$U(x) = \frac{g_0^2 \Delta_a}{\gamma^2 + \Delta_a^2} \cos^2(k_c x) = U_0 \cos^2(k_c x) \propto \chi'. \tag{5.10}$$

The atom is a dispersive and absorbing medium. Thus it changes the electric field amplitude according to the complex susceptibility $\chi = \chi' - i\chi''$ and the linear polarization $P = \epsilon_0 \chi E$. The real part of the susceptibility refers to the absorption of the medium, which is a Lorentzian curve around the atomic transition frequency, broadened by the spontaneous emission rate. The amplitude of the absorption depends on the atomic position because the interaction strength modulates with the spacial dependent cavity mode function $f_L(x)$. The imaginary part of the susceptibility refers to the absorption coefficient of the medium. It is also a Lorentzian and implies that these effects are maximum at positions of maximal cavity field intensity, which are the anti nodes $kx = n\pi$ for $n \in \mathbb{Z}$.
If we reset the operator in (5.3) for the expectation values and put this into the Hamiltonian, we get

$$H_{eff} = -[\Delta_c - U(x)]a^\dagger a + i[\eta_{eff}(x,t)a^\dagger - \eta^*_{eff}(x,t)a] \tag{5.11}$$

with $\eta_{eff}(x,t) = \eta_L + \tilde{\eta}_T(x,t)$. The energy of the cavity field varies in space with $U(x)$ and the effective total pump creates a field (coherent state) that varies around the value of the longitudinal pump in time and the strength of this modulation also depends on the atomic position.
The force on the motionless atom is

$$f = i[H,p] = -\nabla g f_L(x)(\sigma_+ a + a^\dagger \sigma_-) \tag{5.12}$$

$$= -\nabla U(x) a^\dagger a - \nabla[\tilde{\eta}_T(x,t)a^\dagger - \tilde{\eta}^*_T(x,t)a] \tag{5.13}$$

$$= f_1 + f_2. \tag{5.14}$$

The force can also be derived in a complete classical treatment of an atomic dipole oscillating in the standing wave inside the cavity [6]. For $\Delta_a < 0$, $f_1$ traps the atom at intensity maxima ("hight field seeker"), while for $\Delta_a > 0$ the atom gets trapped at intensity minima ("low field seeker"). When the transverse pump strength increases, the force $f_2$ can become strong enough to cancel $f_1$ out, due to their different dependencies on $x$. But since the forces still depend on the photon numbers and field amplitudes here, it is more convenient to do the detailed analysis of the rival forces in the steady-state case for the atom and the cavity field.

## 5.2 Bad cavity limit

For cavity loss rates that fulfill $\kappa \gg \{g(x), \eta_L\}$ the cavity field follows the time evolution of the atom adiabatically and we can eliminate the field variables

$$\dot{a} \simeq 0 \Rightarrow a \simeq \frac{-g(x)\sigma_- + \eta_L}{\kappa - i\Delta_c}. \tag{5.15}$$

The equation of motion for the atomic polarization analog to the dispersive limit (good cavity regime) is

$$\dot{\sigma}_- \simeq [-\gamma - \kappa(x) + i(\Delta_a - \tilde{U}(x)]\sigma_- + \tilde{\eta}_L(x) + \eta_T e^{i\Delta_T t} \tag{5.16}$$

with

$$\tilde{\eta}_L(x) = \frac{g(x)\eta_L}{\sqrt{\kappa^2 + \Delta_c^2}} e^{i\psi} \tag{5.17}$$

for $\psi = -\arctan\frac{\kappa}{\Delta_c}$ and

$$\tilde{U}(x) = \frac{g_0^2\Delta_c}{\kappa^2 + \Delta_c^2}\cos^2(k_c x) \qquad \kappa(x) = \frac{g_0^2\kappa}{\kappa^2 + \Delta_c^2}\cos^2(k_c x). \tag{5.18}$$

The atomic transition experiences a Stark-shift by the external electric field depending on the atomic position, a spatial dependent longitudinal pump rate adds to the transverse one and an effective spatial dependent cavity loss rate adds to the spontaneous emission rate.

## 5.3 Steady-state forces

In order to get an analytic expression for the total force we want to eliminate both $\alpha$ and $\beta$ in the steady state. If we eliminate both operators we suggest far off-resonant drivings. All expectation values of operator products separate in this limit [6] so it is purely classical.
The most convenient way to calculate the properties of the steady-state is to define Eq. (5.2) in matrix notation

$$\dot{\vec{X}} = A\vec{X} + \vec{Y} \tag{5.19}$$

where

$$\vec{X} = \begin{pmatrix}\alpha\\ \beta\end{pmatrix}, \qquad A = \begin{pmatrix} -(\kappa - i\Delta_c) & -g(x) \\ g(x) & -(\gamma - i\Delta_a)\end{pmatrix}, \qquad \vec{Y} = \begin{pmatrix}\eta_L \\ \eta_T e^{i\Delta_T t}.\end{pmatrix} \tag{5.20}$$

Analog to (5.6) we define $\kappa + i\Delta_c = c_2 e^{i\psi}$ and write the diagonal elements of $A$ in polar coordinates

$$A = -\begin{pmatrix} c_2 e^{-i\psi} & g(x) \\ -g(x) & c_1 e^{-i\phi}.\end{pmatrix} \tag{5.21}$$

The steady-state condition gives

$$A\vec{X} = -\vec{Y} \Rightarrow \vec{X} = -A^{-1}\vec{Y}. \tag{5.22}$$

The two by two matrix can be easily inverted and we get

$$\begin{pmatrix}\alpha\\ \beta\end{pmatrix} = \begin{pmatrix} c_2e^{-i\psi} & g(x) \\ -g(x) & c_1e^{-i\phi}\end{pmatrix}^{-1}\begin{pmatrix}\eta_L\\ \eta_T e^{i\Delta_T t}\end{pmatrix} \tag{5.23}$$

$$= \frac{1}{\det A}\begin{pmatrix} c_1e^{-i\psi} & -g(x) \\ g(x) & c_2e^{-i\phi}\end{pmatrix}\begin{pmatrix}\eta_L\\ \eta_T e^{i\Delta_T t}\end{pmatrix} \tag{5.24}$$

$$= \frac{1}{\det A}\begin{pmatrix}\eta_L c_1 e^{-i\phi} - g(x)\eta_T e^{i\Delta_T t}\\ c_2\eta_T e^{i(\Delta_T t-\psi)} + g(x)\eta_L\end{pmatrix} \tag{5.25}$$

where

$$\begin{aligned}\det A &= c_1c_2e^{-i(\phi+\psi)} + g^2(x)\\ &= \kappa\gamma - \Delta_a\Delta_c - i(\kappa\Delta_a + \gamma\Delta_c) + g^2(x).\end{aligned} \tag{5.26}$$

Now we have to calculate the product $2\beta^*\alpha$ and take the imaginary part in order to determine the force:

$$2Im\{\beta^*\alpha\} = \frac{2}{|\det A|^2}Im\{(c_2\eta_T e^{-i(\Delta_T-\psi)} + g(x)\eta_L)(c_1\eta_L e^{-i\phi} - g(x)\eta_T e^{i\Delta_T t})\} \tag{5.27}$$

$$\begin{aligned}=&\frac{2}{|\det A|^2}Im\{c_1c_2\eta_L\eta_T e^{-i(\Delta_T+\phi-\psi)} - g(x)c_2\eta_T^2 e^{i\psi}\\ &+ g(x)c_1\eta_L^2 e^{-i\phi} - g^2(x)\eta_L\eta_T e^{i\Delta_T t}\}\end{aligned} \tag{5.28}$$

$$\begin{aligned}=&\frac{2}{|\det A|^2}[g(x)(\eta_L^2\Delta_a - \eta_T^2\Delta_c)\\ &+ \eta_L\eta_T((\gamma\Delta_c - \kappa\Delta_a)\cos(\Delta_T t) - (\gamma\kappa + \Delta_a\Delta_c - g^2(x))\sin(\Delta_T t)].\end{aligned} \tag{5.29}$$

The denominator is

$$|\det A|^2 = (\kappa^2 + \Delta_c^2)(\gamma^2 + \Delta_a^2) + 2g^2(x)(\kappa\gamma - \Delta_c\Delta_a) + g^4(x). \tag{5.30}$$

The total force consists of two components:

$$f_{total} = f_1 + f_2 \tag{5.31}$$

$$f_1 = \frac{\nabla g^2(x)}{|\det A|^2}(\eta_L^2\Delta_a - \eta_T^2\Delta_c) \tag{5.32}$$

$$f_2 = \frac{2g'(x)}{|\det A|^2}\eta_L\eta_T((\gamma\Delta_c - \kappa\Delta_a)\cos(\Delta_T t) - (\gamma\kappa + \Delta_a\Delta_c - g^2(x))\sin(\Delta_T t)). \tag{5.33}$$

The force $f_1$ refers to the intensity dependent optical trapping that always occurs for the single pump setup. If one of the pump rates is zero the second force gives the optical trap where the amplitude is proportional to the field intensity. For the double pump scheme the intensity gets modified to a sum of both pump rates, where the components are weighted with the detunings. The forces $f_2$ arises from the interference of the longitudinal beam and the transverse photons, that scatter on the atom into the cavity. Due to their frequency difference, the superposition of both fields shows a beating with $\Delta_T$ in time. Their amplitudes vanish if one of the two pump rates is zero. The shift of the resonance frequencies appears in the last term.

## 5.4 Reduction to a perturbed oscillator

In the parameter regime of large detunings, where the steady state solution is valid, terms consisting of products of the cavity parameters will highly overrate the spatial dependent coupling terms. We want to consider the case where the spatial dependency in the denominator and the frequency shift in the interference force $f_2$ are negligible, i.e. we approximate

$$|\det A|^2 \approx (\kappa^2 + \Delta_c^2)(\gamma^2 + \Delta_a^2) \tag{5.34}$$

$$f_2(x,t) \approx -\frac{2g'(x)\eta_L\eta_T}{|\det A|^2}(\gamma\kappa + \Delta_a\Delta_c)\sin(\Delta_T t) \tag{5.35}$$

where we assumed $\Delta_a \gg \{\gamma, \kappa\}$. With use of the canonical equations

$$\dot{p} = f_1(x) + f_2(x,t) = -\frac{\partial H(x,p,t)}{\partial x} \tag{5.36}$$

$$\dot{x} = 2\omega_r p = \frac{\partial H(x,p,t)}{\partial p} \tag{5.37}$$

the system can be described by the Hamilton function

$$H(x,p,t) = \omega_r p^2 - a\cos^2(kx) + b\sin(\Delta_T t)\cos(kx). \tag{5.38}$$

We identify the amplitudes

$$a = \frac{g_0^2(\eta_L^2\Delta_a - \eta_T^2\Delta_c)}{(\kappa^2 + \Delta_c^2)(\gamma^2 + \Delta_a^2)} \qquad b = \frac{2g_0\eta_L\eta_T(\gamma\kappa + \Delta_a\Delta_c)}{(\kappa^2 + \Delta_c^2)(\gamma^2 + \Delta_a^2)}. \tag{5.39}$$

This is the Hamilton function of a nonlinear oscillator with a time and spatial dependent perturbation. The size of the pump rates $\eta_L$ and $\eta_T$ determines the strength of both amplitudes $a$ and $b$.

We want to approximate the trap frequencies of the two forces for the case of good localizations in the potential minima. We can expand the time independent potential so that the unperturbed part of the Hamilton function becomes

$$H_0 = \omega_r p^2 - a\cos^2(kx) \approx \omega_r p^2 + a(x^2 - 1). \tag{5.40}$$

This leads to an equation of motion for the unperturbed system

$$\ddot{x} = -4\omega_r a x \tag{5.41}$$

with an oscillation frequency $\omega_0 = 2\sqrt{\omega_r a}$.

The maximum trap frequency of the perturbation part can be obtained by $\cos(x) \approx -1 + \frac{x^2}{2}$ around a minimum, leading to $\ddot{x} = -2\omega_r b x$ and a maximum trap frequency of the perturbation $\omega_0' = \sqrt{2\omega_r b}$.

The perturbed oscillator is a typical example of a Hamiltonian system that can show chaotic dynamics. The exact oscillation frequency for given initial conditions $\omega_0(x_0, p_0)$ can be calculated via elliptic integrals [40]. The ratio between this frequency and the frequency of the oscillation in time of the perturbation is important for the resulting motion of the oscillator. If the ratio is a

rational number nonlinear resonances occur [38]. For irrational ratios some trajectories remain periodic under perturbation, referring to the KAM-theorem [42].
Unfortunately we cannot to go into details of nonlinear dynamics here but it is important to point out that the chaotic motion of the perturbed pendulum close to the separatrix might be the explanation for the random character of the motion we observe in our system. For a nonlinear oscillator or pendulum with an amplitude close to the separatrix the perturbation might force the system to make a loop or it also might prevent it from undergoing a loop if the perturbation is applied at the right time. This leads to an unpredictable motion of the perturbed pendulum for initial conditions inside the stochastic layer [40]. The regime we see in Fig. 3.4 might be identified with the case $b \gg a$, i.e. an extremely large perturbation where the particle motion is guided by $f_2$ only.

## 5.5 Simplified model without back-action

If we suggest a small coupling with respect to the detunings, the damping rates and the pump rates, we can simplify the equations of motion for the expectation values $\alpha$ and $\beta$ crucially by crossing the back action terms in each equation. The remaining equations are not coupled to the atomic position any more, so they can be integrated. By this step we neglect any dispersive effect of the atom on the cavity field. The system of differential equations becomes

$$\dot{x} = 2\omega_r p \tag{5.42}$$
$$\dot{p} = g'(x) 2Im\{\beta^* \alpha\} \tag{5.43}$$
$$\dot{\alpha} = (-\kappa + i\Delta_c)\alpha + \eta_L \tag{5.44}$$
$$\dot{\beta} = (-\gamma + i\Delta_a)\beta + \eta_T e^{i\Delta_T t}. \tag{5.45}$$

Now we integrate (5.44)and (5.45):

$$\alpha(t) = \alpha_0 e^{(-\kappa + i\Delta_c)t} + \eta_L \int_0^t e^{(-\kappa + i\Delta_c)(t-t')} dt' \tag{5.46}$$
$$= \alpha_0 e^{(-\kappa + i\Delta_c)t} + \frac{\eta_L}{\kappa - i\Delta_c}(1 - e^{(-\kappa + i\Delta_c)t}) \tag{5.47}$$
$$= \{\alpha_0 + \frac{\eta_L}{-\kappa + i\Delta_c}\} e^{(-\kappa + i\Delta_c)t} + \frac{\eta_L}{\kappa - i\Delta_c} \tag{5.48}$$
$$\beta(t) = \beta_0 e^{(-\gamma + i\Delta_a)t} + \eta_T \int_0^t e^{(-\gamma + i\Delta_a)(t-t')} e^{i\Delta_T t'} dt' \tag{5.49}$$
$$= \{\beta_0 + \frac{\eta_T}{\gamma - i\Omega}(e^{(\gamma - i\Omega)t} - 1)\} e^{(-\gamma + i\Delta_a)t} \tag{5.50}$$
$$= \{\beta_0 + \frac{\eta_T}{-\gamma + i\Omega}\} e^{(-\gamma + i\Delta_a)t} + \frac{\eta_T}{\gamma - i\Omega} e^{i\Delta_T t} \tag{5.51}$$

with $\Omega = \omega_T - \omega_a$.
We want to look at times where the damping terms are negligible, i.e. $t > t_0$ where $\{e^{-\gamma t}, e^{-\kappa t}\} \ll 1$. The first term in both equations drop since they decay exponentially. This gives us more sim-

ple expressions

$$\alpha = \frac{\eta_L}{\kappa - i\Delta_c} \tag{5.52}$$

$$\beta(t) = \frac{\eta_T}{\gamma - i\Omega} e^{i\Delta_T t} \tag{5.53}$$

leading to the force

$$f(x,t) = 2g'(x) Im\{\beta^* \alpha\} \tag{5.54}$$

$$= \frac{2g'(x)\eta_L\eta_T}{(\kappa^2 + \Delta_c^2)(\gamma^2 + \Omega^2)} Im\{(\gamma - i\Omega)(\kappa + i\Delta_c)e^{-i\Delta_T t}\} \tag{5.55}$$

$$= \frac{2g'(x)\eta_L\eta_T}{(\kappa^2 + \Delta_c^2)(\gamma^2 + \Omega^2)} ((\gamma\Delta_c - \kappa\Omega)\cos(\Delta_T t) - (\gamma\kappa + \Delta_c\Omega)\sin(\Delta_T t)) \tag{5.56}$$

for $\Omega \approx \Delta_a$ and $\Delta_a \ll \{\gamma, \kappa\}$ we get

$$f(x,t) \approx \frac{2g'(x)\eta_L\eta_T}{(\kappa^2 + \Delta_c^2)(\gamma^2 + \Delta_a^2)} (\gamma\kappa + \Delta_c\Delta_a)\sin(\Delta_T t) \tag{5.57}$$

which is the same force as (5.35). Thus we demonstrated an alternative way to derive the force in the regime of Fig. 3.4.

# Chapter 6

# Numerical results

In this chapter we try to find numerical evidence for the observed random walk behavior of the particle motion by calculating statistical quantities that characterize a random walk in general. As discussed in chapter 4 the final distribution over a one dimensional equidistant lattice should be a binomial distribution that coincides with a Gaussian curve for large times and the variance in space should increase linearly in time. Since the motion of the particle samples harmonic oscillations during one trapping period the interesting quantity to observe is the jump pattern of a trajectory between potential wells at different positions. If the particle walks randomly on the trapping sites the direction in which a jump to the next potential minimum occurs should be completely random, i.e. the probabilities for jumping to the left and right should be one half each and the auto-correlation function of the jump pattern should be delta- correlated.
Before we simulate the system for a large amount of different initial values we test if the analytical results for the simplified model coincide with the numerical solutions. Then we discuss the procedure of the discretization of a single trajectory and how we calculate the correlation function of a jump pattern.

## 6.1 Comparison with analytical solutions

The numerical investigations in this chapter are accomplished in a parameter regime where the cavity field and the atomic polarization are basically uncoupled as discussed in the simplified model without back-action so the coupling constant $g$ is small with respect to the detuning parameters and the pump rates. This model already seems to coincide with the parameter regime used in chapter 3 for a transverse pump rate of $\eta_T = 0.5$ since the potential, plotted as the colored background of Fig. 3.5a), is of the shape of a cosine in space times a sine in time and that is also the result of the analytical calculation of the force in the simplified model without back-action Eq. (5.57). To make the approximation of crossing the back-action even more valid we choose a lower coupling constant than in chapter 3 and also increase the transverse pump rate to get a larger potential amplitude. Additionally we use detunings and decay rates for that we can be shure that the phase in the time dependency of the force Eq. (5.56) disappears and we get a pure sine modulation in time, i.e. $\gamma\Delta_c = \kappa\Delta_a$.

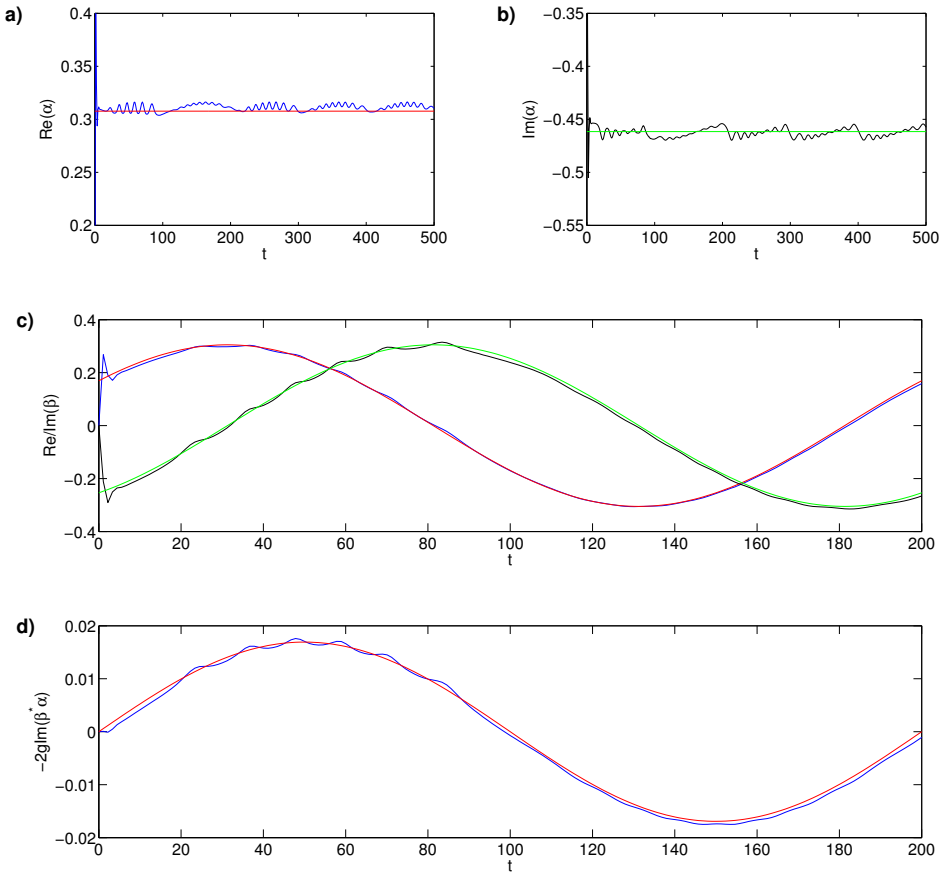


Figure 6.1: Fit of the numerical solutions with the analytic solutions from section 5.5 for parameters $\gamma = 1.0$, $g = 5 \times 10^{-2}$, $\Delta_a = -1.5$, $\Delta_c = -1.5$, $\eta_L = 1$, $\eta_T = 0.55$, $T = 100$, $\omega_r = 0.1$, $k = 2\pi$ and initial values $x_0 = 3.4913 \times 10^{-3}$ and $p_0 = \alpha_0 = \beta_0 = 0$. For these parameters we get a ratio between the two amplitudes in (5.39) of $\frac{b}{a} = 34.17$. a)-c) The numerical solutions oscillate around the analytical with small deviations. a)Real part of the field amplitude with numerical(blue) and analytical(red) solution. b) Imaginary part of the field amplitude with numerical(black) and analytical(green) solution. c) Real and imaginary part of the polarization amplitude with the same color pattern as for $\alpha$ in a) and b). d) Modulation of the force in time at the position $x = \frac{1}{4}$. As before the numerical solution(blue) oscillates slightly around the analytical one(red) guided by a sinusoidal oscillation with period $\frac{2\pi}{\Delta_T} = 200$.

## 6.2 Discretization of a single trajectory

The period $T = \frac{\pi}{\Delta_T}$ with which the jumps occur is half of the period of the potentials oscillation in time. Over one jump-period $T$ the trajectory is reduced to it's mean value, rounded on an integer or half integer value that is constant over one half period in time, i.e.

$$x_n = [\frac{2}{T}\int_{nT}^{(n+1)T} x(t)dt]/2. \tag{6.1}$$

Now the series of positions $\{x_n\}_{n=0}^{N}$ is an array of the minima of the potential wells, in which the particle is trapped. At these positions the force that acts on the particle is always zero.
The jump direction is registered by subtracting two adjacent steps from each other and dividing the difference by the absolute distance of the jump to normalize the entry to one. We define a single jump $j_n$ and a set of $N-1$ jumps $J_N$ as

$$j_n = \frac{x_n - x_{n-1}}{|x_n - x_{n-1}|} \qquad J_N = (j_1, j_2, \ldots, j_{N-1}). \tag{6.2}$$

The resulting function describes a trajectory as a sequence of plus and minus signs, where we write a plus for positive jumps to the right and a minus for negative jumps to the left.
The auto-correlation function of such a set $J_N$ is defined as

$$C(\tau) = \lim_{N\to\infty} \frac{1}{N-1}\sum_{n=1}^{N}(j_{n+\tau} - \langle j_n\rangle)(j_n - \langle j_n\rangle). \tag{6.3}$$

The two point auto-correlation function measures how much two magnitudes are related to each other in dependency of the distance in time. In our case, it shows how a jump at one time step influences the direction of the jump at some other time. When they are uncorrelated, the system has no memory about it's earlier behavior. Negative correlation means in our case that it is probable at the given distance to have a jump into the direction opposite to the direction of the jump at the distance zero. Since we can not perform the limit $N \to \infty$ we always have less data for the mean value that gives us the correlation at larger distances than for short distance. Because of that the number of steps should always be large against the range of distances $\tau$ we are looking at when we calculate the correlation numerically.

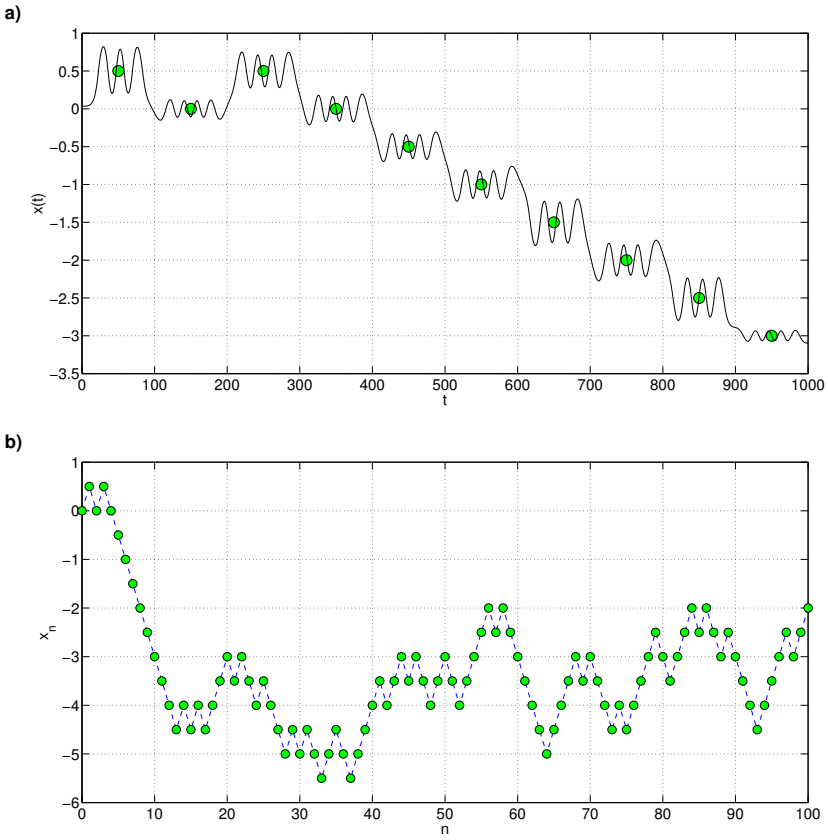


Figure 6.2: Discretized trajectory. a) The first ten jumps of a continuous curve are reduced to a sequence of discrete positions (green dots) at times $t_n = \frac{2n+1}{2}T, n \in \mathbb{N}_0$. b) Full discrete curve with $10^2$ entries.

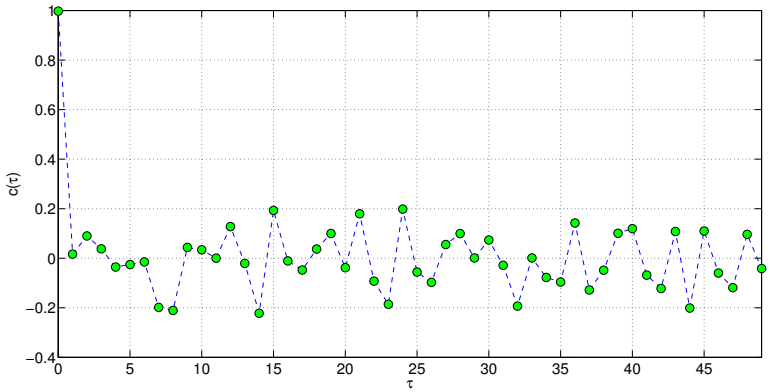


Figure 6.3: Correlation function for the discrete curve of Fig. 6.2b). The function has a value of one at distance zero and fluctuates around zero for all other distances.

## 6.3 Many trajectories statistics

We solved the system numerically for $10^3$ different initial values that are created by a pseudo-random number generator and lie in the square interval $(x_0, p_0) \in [-0.1, 0.1] \times [-0.1, 0.1]$. Each trajectory starts in the discrete position zero, but the small differences in the initial conditions generate different evolutions in time. All trajectories are visualized in one figure with green lines for an initial position $x_0 > 0$ and black for $x_0 < 0$. For uncorrelated particle motion the colored curves would mix in the way, that there are no regions where one color dominates.
The final distribution of the end positions of all trajectories after $10^2$ jumps is filled into an histogram where we expect a binomial distribution with mean zero. We also fit a continuous Gaussian distribution as black curve on the histogram with a standard deviation estimated from the end positions of all trajectories.
Further we calculate the variance in position as a function of $n$. According to Chapter 4 the variance for a discrete one dimensional random walk starting at zero without a drift is

$$\left\langle (\Delta x)^2 \right\rangle = 4 \frac{pqa^2}{T} t. \tag{6.4}$$

The mean initial values $\langle x_0 \rangle$ and $\langle p_0 \rangle$ are very close to zero so we expect distributions around zero and no drift velocity. The lattice constant of our system is $a = \frac{1}{2}$ and the time variable is discretized by $t = nT$. So we get $\langle (\Delta x_n)^2 \rangle = \frac{1}{4} n$ for $p = q = \frac{1}{2}$.
At last we calculate the mean correlation function of the ensemble of single trajectories. Compared to the correlation function of a single curve the fluctuations should be reduced. Although we modified the parameters for better trapping by the interference force, it might happen that the particle jumps over more than one lattice side and the calculation of the discrete position as a mean value gives twice the same result for adjacent locations. In the latter case, the $j_n$ is divided by zero so the correlation function has singularities that we have to delete. To get rid of the singularities we pick out all trajectories that have jumps of size zero and set the correlation for these single curves to zero for distances larger than zero.
In order to observe changes in the statistics of the system we vary the beating frequency in five steps while leaving all other parameters constant.
The particle oscillates more times inside a well if the beating period is larger. We want to test if more oscillations lead to a higher loss of memory and the particle motion gets less correlated. Like in Brownian motion an increase of the time scale we are looking at means that the particle gets kicked more often and the direction of it's movement after larger times is less predictable. On the other hand we can say, that independent of the length of the beating period, the motion of the particle during one period of oscillation of the potential follows the same rule and does not get more complicated, it just oscillates a few times more. For this case some values of the beating period might match with the properties of harmonic oscillations of the particle in a way that jumps into one direction are more probable after a some amount of beating periods than jumps into the other direction. This would lead to oscillations in the correlation function. Again a detailed analysis of this question requires a deep excursion into nonlinear dynamics and it's connection to stochastic processes.

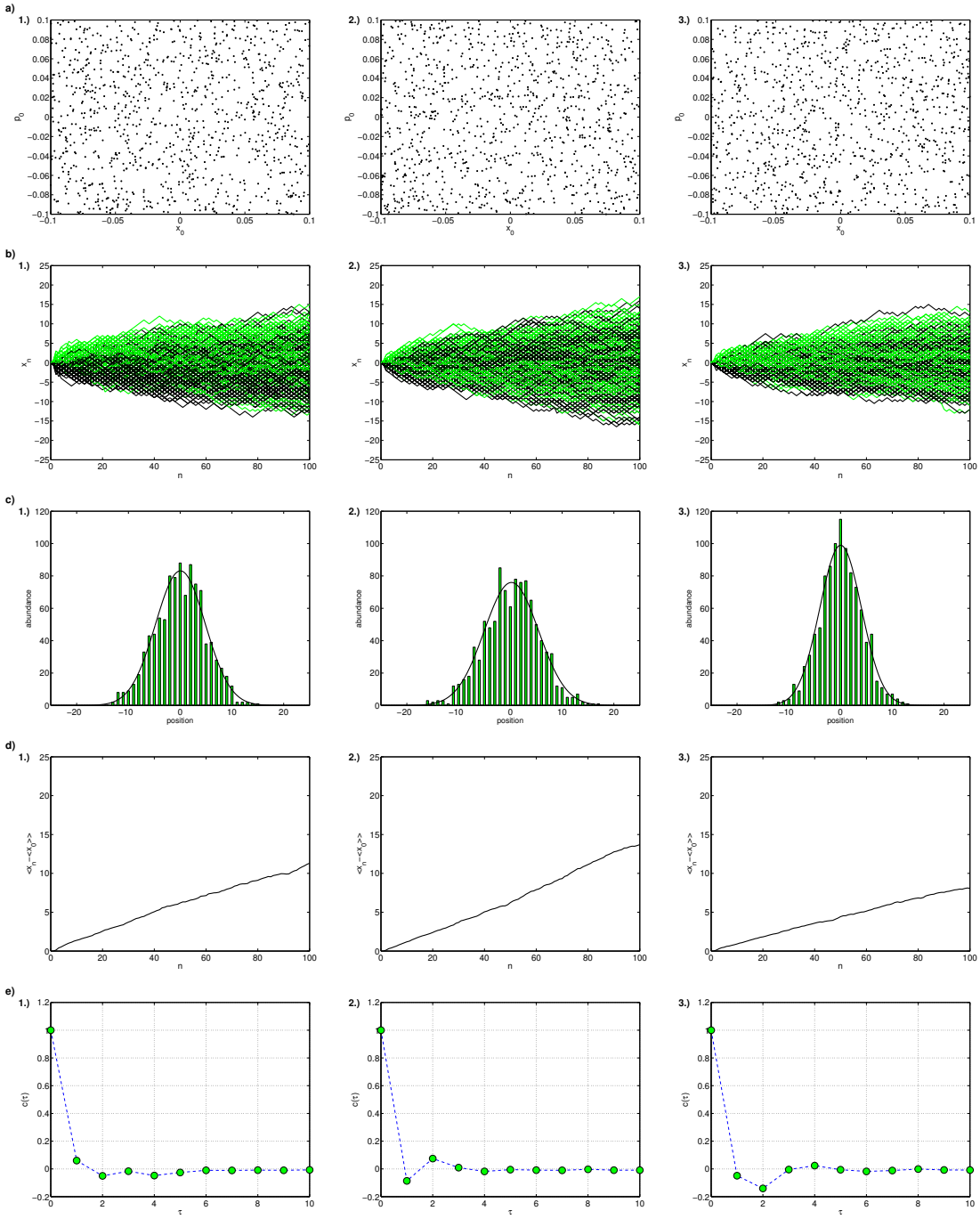


Figure 6.4: Simulation of $10^3$ trajectories for $T = 100$, $T = 150$ and $T = 200$. a) Random initial values used in the simulation. b) Mixing of the trajectories. We also that the trajectories spread more or less due to different diffusion constants. c) Histograms of the final positions after $10^2$ steps. All simulations end up with Gaussian distributed positions where the width depends on the beating frequency. d) Variance in $x$. The slope of the variance is equivalent to the diffusion constant and has a maximum value of $0.25$ for a perfect one dimensional random walk. e) Auto-correlation functions of the discretized trajectories. All correlations decay quiet fast but the oscillations around zero vary with the beating period.

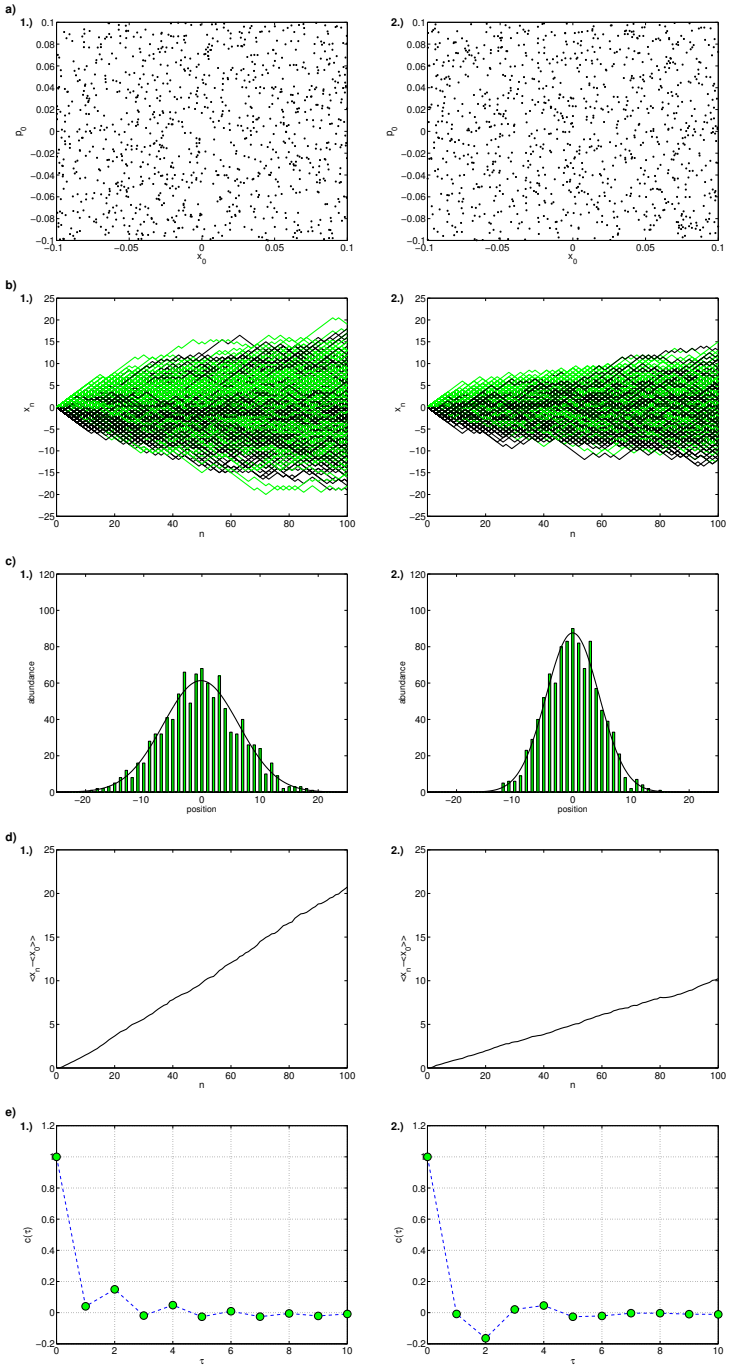


Figure 6.5: Simulation of $10^3$ trajectories with random initial values for $T = 250$ and $T = 300$.

The fact that the slope of the variance does not converge to $0.25$ and the correlation function does not get closer to a delta-function for an increasing beating period speaks against the hypothesis that more oscillations of the particle inside a well leads to a loss of memory and speaks for the theory that the ratio of beating and oscillation period mostly determines the randomness of the system.

## 6.4 Diffusion for non delta-correlated forces

The correlation functions of the jump directions do not perfectly coincide with a delta function around zero for any beating frequency $\Delta_T$. Now we want to investigate how the variance in $x$ as a function of time for a particle looks like, that feels a non delta- correlated force. The explicit shape of the force correlation is inspired by the jump correlation functions we simulated in Fig. 6.4 and 6.5, i.e. a Gaussian distribution functions times a cosine modulation.
In section 4 we assume a particle underlying the equation of motion

$$\frac{dv}{dt} = -\lambda v + \xi(t). \tag{6.5}$$

The variance in space is

$$\left\langle (\Delta x)^2 \right\rangle = \int_0^t dt' \int_0^t dt'' \phi(t')\phi(t'') \left\langle \xi(t')\xi(t'') \right\rangle \tag{6.6}$$

with $\phi(\tau) = \frac{1}{\lambda}(1 - e^{\lambda(t'-t)})$. The correlation function in space can be obtained analytically by changing the upper border of integration in the second integral to some $\bar{t}$.
The expectation value only acts on the force product since $\phi(\tau)$ is independent of the initial values. This gives us the two-time correlation function $\langle \xi\xi \rangle (\tau) = 2dC(\tau)$, consisting of an amplitude, which is two times the velocity-diffusion constant $d$, and a normalized distribution function $C(\tau)$. We have to include the correct normalization over the time distance $\tau = t' - t''$ so that $\int_\infty^\infty d\tau C(\tau) = 1$. With

$$\int_{-\infty}^{\infty} d\tau e^{-\tau^2/2\sigma^2} \cos(\Omega\tau) = \frac{\sqrt{2\pi}\sigma}{e^{\Omega^2\sigma^2/2}} \tag{6.7}$$

we get the correlation function

$$\langle \xi(t')\xi(t'') \rangle = 2d \frac{e^{\Omega^2\sigma^2/2}}{\sqrt{2\pi}\sigma} \cos(\Omega(t' - t'')) e^{(t'-t'')^2/\sigma^2} \tag{6.8}$$

$$\xrightarrow{\sigma,\Omega\to 0} 2d\delta(t' - t'') \tag{6.9}$$

The integration in Eq. (6.6) is done numerically. We set $\Omega = 0$ and vary the width of the Gaussian from $0.1$ to $1$. Then we set $\sigma = 0.5$ and vary $\Omega$ from $\frac{\pi}{5}$ to $2\pi$.

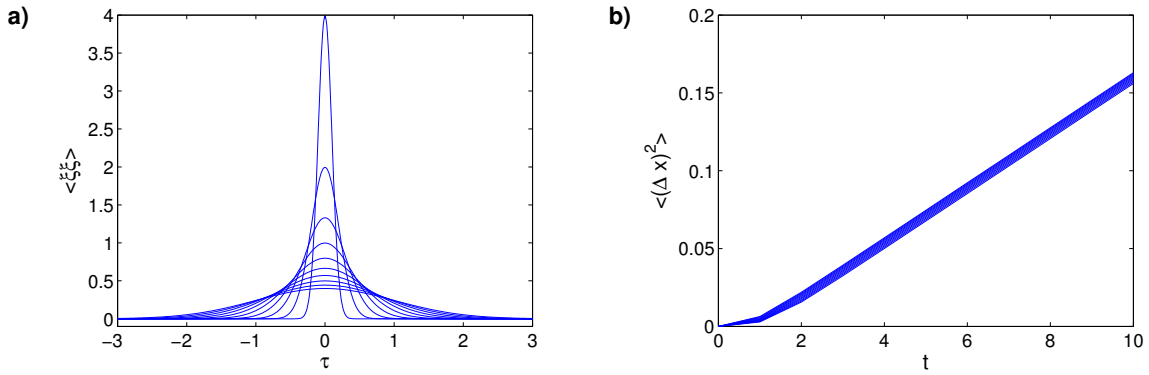


Figure 6.6: Diffusion for the Gaussian correlated force of 6.9 with $\Omega = 0$. a) Shape of the correlation function for $\sigma \in 0.1\{1, 10\}$. b)Variances for the different widths of the correlation. The variance grows below the linear curve through the origin but turns into a linear function with the same slope after short times. This effect gets heavier as $\sigma$ increases and can be seen as an effective horizontal shift of the variance.

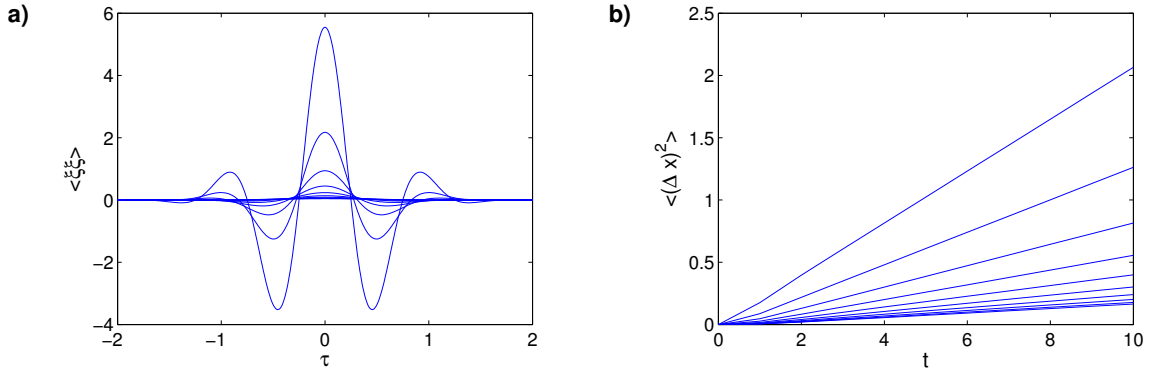


Figure 6.7: Diffusion for the force-correlation of 6.9 with $\sigma = 0.5$. a) Shape of the correlation function for $\Omega \in \frac{\pi}{5}\{1, 10\}$. b)Variances for the different frequencies. The oscillation frequency influences the slope of the variance, i.e. the diffusion constant, strongly. The diffusion decreases with increasing $\Omega$.

The different slopes of the variances in $x$ from our simulations of the systems equations of motion (Fig.6.4 and Fig.6.5)seem to refer to oscillations in the time correlation of the force on the particle. Higher oscillation frequencies seem to induce a smaller diffusion constant so the particle diffusion is slower that for the delta-correlated case.

# Chapter 7

# Model extensions

In the previous calculations we always assumed the low saturation limit. Here we want to demonstrate a way to derive the fifth equation of motion for the saturated atom.
After that we consider the case of a nanoparticle, consisting of many single atoms that have a center of mass motion and derive the equations of motion with the Tavis-Cummings Hamiltonian. Further we propose a way to construct a famous example for Hamiltonian chaos, namely the kicked rotor, out of our system.

## 7.1 Saturated single atom

The occupation of the excited state of a single two level atom is restricted to one. Now we want to leave the low saturation limit and allow arbitrary occupations between zero and one. In this case the atomic operator $\hat{\sigma}_z$, which measures the electronic state of the atom evolves in time and introduces an additional degree of freedom to our system.
The quantum Langevin equation for the atomic annihilation operator $\hat{\sigma}^-$ is

$$\dot{\sigma}^- = (-\gamma + i\Delta_a)\sigma^- - gf(x)\sigma_z a - \eta_T \sigma_z e^{i\Delta_T t} + F_2 \tag{7.1}$$

Again we take the expectation values, assume that all operator products separate, define $\beta = \langle\hat{\sigma}^-\rangle$ and $\beta_z = \langle\hat{\sigma}_z\rangle$ and get the equations of motion in the frame rotating with $\omega_L$

$$\dot{\beta} = (-\gamma + i\Delta_a)\beta - gf(x)\beta_z\alpha - \eta_T\beta_z e^{-i\Delta_T t}. \tag{7.2}$$

Now we calculate the time evolution of $\beta_z$ as the trace over the time evolution of the density matrix:

$$\begin{aligned} \beta_z &= \mathrm{Tr}[\rho\dot{\sigma}_z] = \mathrm{Tr}[\dot{\rho}\sigma_z] && (7.3)\\ &= \mathrm{Tr}[\sigma_z(-i[H_{tot},\rho] + \mathcal{L}\rho)]. && (7.4) \end{aligned}$$

The first term is

$$\begin{aligned} -\mathrm{Tr}[\sigma_z i[H_{tot},\rho]] &= -i\mathrm{Tr}[\sigma_z H_{tot}\rho - \sigma_z\rho H_{tot}] && (7.5)\\ &= -\mathrm{Tr}[\rho[\sigma_z, H_{tot}]] && (7.6) \end{aligned}$$

where we used the cyclic property of the trace. Only the interaction term and the atomic pump do not commute with $\sigma_z$. With $[\sigma_z, \sigma_\pm] = \pm 2\sigma_\pm$ we get

$$-i\text{Tr}[\rho[\sigma_z, H_{tot}]] = \text{Tr}[\rho(2gf(x)(\sigma_+ a + a^\dagger \sigma_-) + 2\eta_T(\sigma_+ e^{i\Delta_T t} + \sigma_- e^{-i\Delta_T t}))] \tag{7.7}$$

$$= 2g\left\langle f(x)(\sigma_+ a + a^\dagger \sigma_-)\right\rangle + 2\eta_T\left\langle(\sigma_+ e^{i\Delta_T t} + \sigma_- e^{-i\Delta_T t})\right\rangle \tag{7.8}$$

$$= 4gf(x)Re\{\beta^*\alpha\} + 4\eta_T Re\{\beta e^{-\Delta_T}\}. \tag{7.9}$$

The second term is

$$\text{Tr}[\sigma_z \mathcal{L}\rho] = 2\gamma\text{Tr}[\sigma_z\sigma_-\rho\sigma_+] - \gamma\text{Tr}[\sigma_z\sigma_+\sigma_-\rho] - \gamma\text{Tr}[\sigma_z\rho\sigma_+\sigma_-] \tag{7.10}$$

$$= -\gamma\left\langle\sigma_+\sigma_-\right\rangle \tag{7.11}$$

$$= -2\gamma\left\langle\sigma_z + \mathbb{1}\right\rangle. \tag{7.12}$$

In conclusion the time evolution of $\beta_z$ is

$$\dot{\beta}_z = -2\gamma(\beta_z + 1) + 4gf(x)Re\{\beta^*\alpha\} + 4\eta_T Re\{\beta e^{-i\Delta_T t}\}. \tag{7.13}$$

Depending on the value of $\beta_Z$ we might get a different behavior of our system. The influence of the additional equation might be tested by solving the set of differential equations Eq. (3.4)-(3.6), (7.2) and (7.13) numerically.

## 7.2 Doped nanoparticles

It is possible to launch particles of the size about $1 - 10^3$nm out of a surface and into a high vacuum cavity [18] by e.g. shooting laser pulses on a silicon wafer that crack out nanoparticles by thermo-mechanical stress. As we have seen, the cavity cooling mechanism is not restricted to two level atoms. In fact any small enough polarizable particle can induce the dispersive shift of the cavity resonance and thus can be cooled.
Apart from this we consider a doped nanoparticle, i.e. a spherical arrangement of atoms doped with a controllable amount of two level atoms, where the driving is slightly detuned with respect to this two-level transition. The advantage of such a doped nanoparticle for our model is that the polarization of the whole sphere can be large since the single atomic polarizations add up, although each single atom is unsaturated. The low saturation condition in this case requires that the number of saturated atoms is much smaller than the total number of atoms of the sphere. The system can be described by the Hamiltonian $H_{tot} = H_0 + H_{TC} + H_{p,a} + H_{p,\sigma}$, consisting of the terms

$$H_0 = \frac{P^2}{2M} + \sum_{i=1}^{N} \omega_a \sigma_i^+ \sigma_i^- + \omega_c a^\dagger a \tag{7.14}$$

$$H_{TC} = igf(x)\sum_{i=1}^{N}(\sigma_i^+ a - a^\dagger \sigma_i^-) \tag{7.15}$$

$$H_{p,\sigma} = i\eta_T \sum_{i=1}^{N}(\sigma_i^+ e^{-i\omega_T t} - \sigma_i^- e^{i\omega_T t}) \tag{7.16}$$

where $P$ and $M$ are momentum and mass of the whole sphere. $H_{TC}$ is known as the Tavis-Cummings Hamiltonian. The expression for $H_{p,a}$ remains the same as in the single atom case. The index $i$ counts the operators acting on the $i$th atom. We define the collective atomic operators $S^{\pm} = \sum_{i=1}^{N} \sigma_i^{\pm}$ and $S_z = \sum_{i=1}^{N} \sigma_{z,i} \simeq -N$. Therefore the Quantum Langevin Equations of our systems operators are

$$\dot{a} = \frac{i}{\hbar}[H_{tot}, a] - \kappa a + F_1, \tag{7.17}$$

$$\dot{S}^{-} = \frac{i}{\hbar}[H_{tot}, S^{-}] - \gamma S^{-} + F_2 \tag{7.18}$$

with noise operators $F_{1,2}$. We take the expectation values of these equations, define $\alpha = \langle a \rangle$ and $\beta = \langle S^{-} \rangle$ and neglect all kinds of quantum correlations. The remaining equations are

$$\dot{\alpha} = (-\kappa + i\Delta_c)\alpha - gf(x)\beta + \eta_L, \tag{7.19}$$

$$\dot{\beta} = (-\gamma + i\Delta_a)\beta + gf(x)N\alpha + \eta_T N e^{i\delta_T t}. \tag{7.20}$$

Since the number of doped particle $N$ is proportional to the back-action term and the transverse pump rate the strength of these terms can be controlled by doping more or less particles of the sphere.

## 7.3 Frequency comb driving

A slightly modified setup allows us to treat the atomic movement in the time dependent potential as an application of the kicked rotor, which is a famous example of nonlinear, chaotic dynamics. The equations of motion of the kicked rotor can be transformed into the two dimensional Chirikov map, also known as the Standard map.
The time dependency in the kicked rotor refers to a Dirac-comb function, that generates the kicks with a certain period. To get this pulse train, we now pump our atom with several transverse lasers of frequencies around the longitudinal one, so that $\Delta_T^{(n)} = n\delta$. The term of the Hamiltonian in the rotating frame pumping the atomic polarization directly is

$$H_{p,\sigma} = i \sum_{n=-N}^{N} \eta_T^{(n)} (\sigma^{+} e^{-i\Delta_T^{(n)} t} - \sigma^{-} e^{i\Delta_T^{(n)} t}). \tag{7.21}$$

The rest of the setup remains is same as in Chapter 5.
The time derivative of the polarization without back action includes the sum over all pumps

$$\dot{\beta} = (-\gamma + i\Delta_a)\beta + \sum_{n} \eta_T^{(n)} e^{i\Delta_T^{(n)}}. \tag{7.22}$$

The integration and calculation of the force is analog to the single transverse frequency driving case in Section 5.5 except of that we have to write a sum over $n$ an the right places. With a negligible low spontaneous emission rate we get the force

$$f = -g'(x) 2 \frac{\eta_L}{c_2} Re\{ie^{-i\psi} \sum_{n} \frac{\eta_T^{(n)}}{\Omega^{(n)}} e^{-i\Delta_T^{(n)} t}\} \tag{7.23}$$

with $c_2 = \kappa^2 + \Delta_c^2$, $\psi = \arctan(\frac{\Delta_c}{\kappa})$ and $\Omega^{(n)} = \omega_T^{(n)} - \omega_a$. When we tune the amplitude of the oscillation in time constant for all $n$, i.e. $\frac{\eta_T^{(n)}}{\Omega^{(n)}} = \hat{\eta}_T$ and modulate the frequencies of the transverse pumps the way that $\Delta_T^{(n)} = n\Delta$ the sum over the complex exponential function of these frequencies in the limit of very large $N$ is the Fourier transformed Dirac-Comb function

$$f \overset{N\to\infty}{=} -g'(x)\frac{\eta_L\hat{\eta_T}}{c_2} Re\{ie^{-i\psi}\sum_{n=-\infty}^{\infty} e^{-in\Delta t}\} \tag{7.24}$$

$$= -g'(x)\frac{\eta_L\hat{\eta}_T}{c_2} Re\{ie^{-i\psi}\}\mathrm{T}\sum_n \delta(t-n\mathrm{T}) \tag{7.25}$$

$$= \underbrace{\frac{g\eta_L\hat{\eta}_T\Delta_c\mathrm{T}}{\kappa^2+\Delta_c^2}}_{=K}\sin(kx)\sum_n \delta(t-n\mathrm{T}) \tag{7.26}$$

where $\mathrm{T} = \frac{2\pi}{\Delta}$ is the period between two kicks. The modulation of the different driving frequencies should be in a small distance around the longitudinal frequency $\omega_T^{(n)} = \omega_L - n\Delta$ and the pump rates should vary like $\eta_T^{(n)} = \hat{\eta}_T(\Delta_a - n\Delta)$ to build the comb function.
In conclusion, our system can be described by the equations of motion

$$\dot{x} = \frac{p}{m} \tag{7.27}$$

$$\dot{p} = K\sin(kx)\sum_n \delta(t-n\mathrm{T}) \tag{7.28}$$

which define the kicked rotor [42]. The amplitude $K$ can be identified with the order parameter for the transition between periodic an chaotic motion for given initial conditions.
We now show how to build the standard map out of (7.27) and (7.28), following the procedure in [42]. A convenient feature of the kicked rotor is the possibility to integrate the equations of motion analytically. The phase space is discretized by

$$[x_n|p_n] = \lim_{\epsilon\to 0}[x(n\mathrm{T}-\epsilon)|p(n\mathrm{T}-\epsilon)]. \tag{7.29}$$

In signal theory, the product of a spacial dependent function times the Dirac comb is an ideal sample [43], that changes a continuous signal into a discrete one, because the product gives zero for all coordinates, that do not belong to the discrete set of points, i.e.

$$f(x)\sum_{n=-\infty}^{\infty}\delta(t-n\mathrm{T}) = \sum_{n=-\infty}^{\infty} f(x_n)\delta(t-n\mathrm{T}) \tag{7.30}$$

for any smooth signal f(x). According to this, the formal integral over (7.28), evaluated at a time between two sequent iteration steps $(n+1)\mathrm{T} > t > n\mathrm{T}$ is

$$p(t) - p_n = \lim_{\epsilon\to 0}\int_{n\mathrm{T}-\epsilon}^{t} dt' \sum_{m=-\infty}^{\infty} K\sin(kx_m)\delta(t'-m\mathrm{T}) \tag{7.31}$$

$$\Leftrightarrow p(t) = p_n + K\sin(kx_n). \tag{7.32}$$

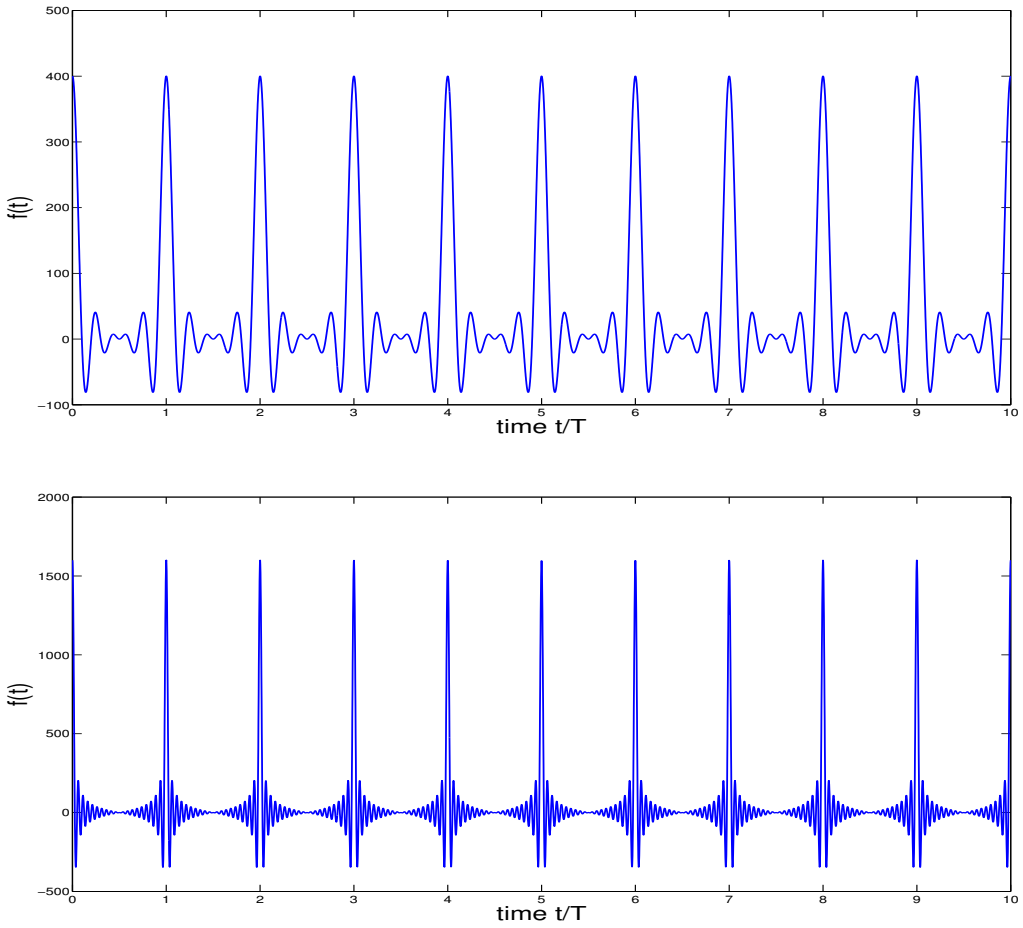


Figure 7.1: The sums over i)$N = 10$ and ii) $N = 40$ cosine modes are plotted for $K = 40.0048$. The Dirac comb has infinitely thin and high peaks at integer multiples of the kicking period. At these positions cosine is equal to one, so the maximal amplitude sums up to the number of used frequencies times the amplitude.

For the x-coordinate we get

$$\dot{x} = \frac{p}{m} \tag{7.33}$$

$$\Rightarrow x(t) - x_n = \lim_{\epsilon \to 0} \int_{n\mathrm{T}-\epsilon}^{t} dt' p(t') \tag{7.34}$$

$$\Leftrightarrow x(t) = x_n + p(t)(t - n\mathrm{T}) \tag{7.35}$$

because p is constant over the integration interval. At the next time step $t = (n+1)\mathrm{T}$ we get the recursive map

$$p_{n+1} = p_n + K \sin(k x_n) \tag{7.36}$$

$$x_{n+1} = x_n + \mathrm{T} p_{n+1}. \tag{7.37}$$

# Chapter 8

# Conclusion and outlook

We considered the dynamics of particles (either as single two-level systems or sub-micron spheres doped with multiple emitters) inside time-dependent potentials resulting from interference in a two-color, two directional pump scheme. Past a given threshold, chaotic-like behavior can be observed, with correlations and position distributions very close to those of a typical random walk. We further calculated the dominating forces in the steady state of the cavity field amplitude and the atomic polarization and reduced the system to a parametrically driven oscillator model, which explains the rise of random dynamics as an instance of deterministic chaos and separates it from dynamics driven by stochastic forces.
The results from the numerical solutions of the system for a large amount of different initial values coincide with our analytical results. They also exhibit particle motion with diffusion constants that are smaller than in the random walk case and we found that this results coincide with the diffusion in Brownian motion with a non delta-correlated force.
Possible expansions of the model to nanoparticles and frequency comb driving were introduced. The logical continuation of our work presented here would be to analyze the parametric driven oscillator model with the Hamiltonian $H = A\cos^2(kx) + B\cos(\Delta_T t)\cos(kx)$ in more detail or relate it to already existing work in that field. We suggest that the analysis with methods of nonlinear dynamics as perturbation theory in $B$, discretization and mapping of the equations of motion or calculating Lyapunov exponents might be promising.
An interesting future perspective could be the evolution of a wave packet inside the time dependent potential. The splitting and re-overlapping of the wave packet would lead to nontrivial interference patterns. One can also thing of this scenario as sort of a quantum random walk since the wave packet clearly has the ability to move to both sides, but it is basically multiple wave interference.
Our work could be useful for research on the influence of the explicit time dependency in the multi particle case and effects of self ordering as mentioned in [10]. The influences of quantum noise should be taken into account as well.
Finally we want to mention some thoughts on the experimental implementation of our system and on the possibility to realize a quantum random walk with the given setup.

## 8.1 Implementation considerations

To observe the proposed quasi random walk experimentally, we propose the following procedure: in a first step, one uses the cavity cooling effect of the longitudinal driving onto an already laser cooled atom (setting $\eta_T = 0$). This corresponds to initializing the atom in a wave packet of energy $\hbar\kappa$ divided between the position and momentum quadrature components. Now we want to calculate the width of this wave-packet.
If we assume that the cavity field and the atomic polarization are in a steady state, we can use our calculations of Section 5.4., where we derived the trapping frequency of the particle inside the time independent optical trap, approximated as a harmonic potential. For an atom that is trapped in the optical potential the energy is described by the harmonic oscillator Hamiltonian

$$H_0 = \omega_r p^2 + a x^2 \tag{8.1}$$

where the recoil frequency is $\omega_r = \frac{\hbar k^2}{2m}$ and the amplitude of the optical potential is given by Eq. (5.39). According to the thermal equipartition principle the minimal energy of the particle $\hbar\kappa$ distributes itself in the two parts

$$\frac{\hbar\kappa}{2} = \hbar\omega_r (\delta p)^2 \qquad\qquad \frac{\hbar\kappa}{2} = \hbar a (\delta x)^2 \tag{8.2}$$

which gives us the variances

$$\delta p = \sqrt{\frac{\kappa}{2\omega_r}} \qquad\qquad \delta x = \sqrt{\frac{\kappa}{2a}}. \tag{8.3}$$

The variance in momentum and space in the correct dimensions are

$$\delta P = \hbar k \sqrt{\frac{\kappa}{2\omega_r}} \qquad\qquad \delta X = \frac{1}{k}\sqrt{\frac{\kappa}{2a}}. \tag{8.4}$$

## 8.2 Applicability for the quantum random walk

A big question in the treatment of the quantum mechanical setup that we describe in Chapter 2 is, if the random walk would be influenced by the internal atomic state if this may lead to a quantum random walk. The brief introduction to the quantum random walk is inspired by [44]. A wave function can, in contrast to a classical particle, walk to the left and right simultaneously. Only when the state is measured the particle has to choose a single position. After more unmeasured steps the wave function interferes with itself and correlations between positions build up, which change the shape of the probability density distribution. If the atomic state is measured after each step, the quantum random walk is the same as the classical, since all correlations are gone after each measurement.
The quantum random walk on a discrete lattice of a wave function $|\psi\rangle = |\psi\rangle_a \otimes |i\rangle$, which is the product state of the atomic wave function and the discrete position $i$, can be described by a unitary operation $U$, which consists of a conditional translation in space and a coin flip. The translation puts the particle to the next position to the left if the atomic state is the ground state,

and makes a translation to the right if the atomic wave function is in the excited state. This is done by the operator

$$S = |e\rangle\langle e| \otimes \sum_i |i+1\rangle\langle i| + |g\rangle\langle g| \otimes \sum_i |i-1\rangle\langle i| \tag{8.5}$$

Additionally the coin flip operator puts the atomic state in a superposition of ground and excited state after each step, which can be done by applying the Hadamard matrix

$$H = \frac{1}{\sqrt{2}} \begin{pmatrix} 1 & 1 \\ 1 & -1 \end{pmatrix} \tag{8.6}$$

Modifying the entries of the coin matrix can weight one atomic state more than the other and make the walk biased. The Hadamard quantum random walk is unbiased or isotropic. Each step of the walk can be calculated by

$$|\psi_{n+1}\rangle = U|\psi_n\rangle = S(H \otimes Id)|\psi_n\rangle. \tag{8.7}$$

With an initial state $|\psi_0\rangle$ the state after $T$ steps is $U^T|\psi_0\rangle$. The spatial probability distribution is observed by projecting on each state in space $|i\rangle$.
An important property of the quantum random walk is the scaling of the variance in space with amount of steps squared, i.e. $\langle(\Delta x)^2\rangle \sim T^2$. The propagation is quadratically faster that in the classical random walk.
For continuous space the step operation has the shape of $e^{2i\sigma_Z \otimes \hat{p}l}$ [45]. The exponential of the momentum operator makes a translation over distance $l$ and the Pauli operator conditions the direction of the translation on the atomic state.

The randomness in the trajectories of our system occurs because of the coupling of two oscillations that are not in phase and the nonlinearities in position. The direction of the particles movement when the potential is down and the jumps happen is not affected by the atomic state.

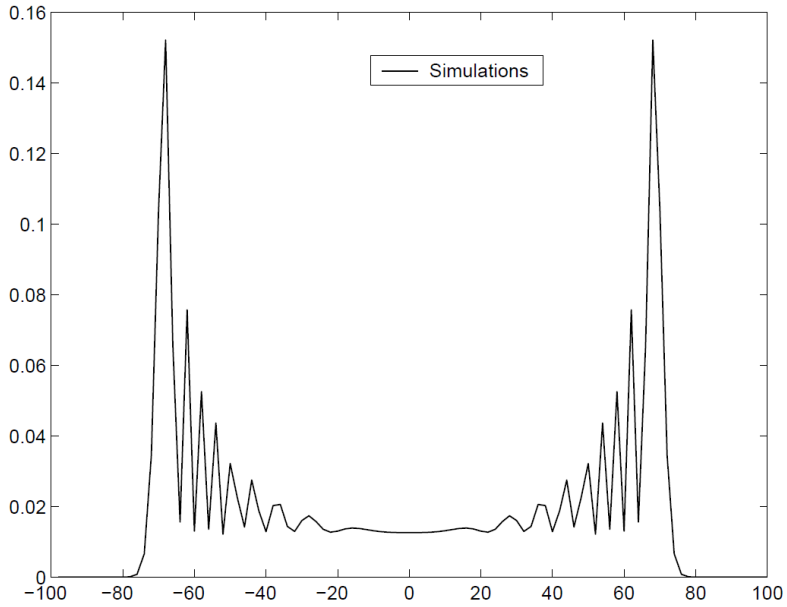


Figure 8.1: Probability distribution of the isotropic discrete quantum random walk with an Hadamard coin and symmetric initial conditions after 100 steps from [44].

# Bibliography


[1] C. Cohen-Tannoudji, Phys. Rep. **209**, Nos.3-6, 153-164 (1992)

[2] J. Dalibart, and C. Cohen-Tannoudji, J. Phys. B., At. Mol. Phys. **18**, 1661-1683 (1985)

[3] H. Mabuchi, Q. A. Turchette, M. S. Chapman, and H. J. Kimble, Opt. Lett. **21**, 1393 (1996)

[4] A. C. Doherty, A. S. Parkins, S. M. Tan, and D. F. Walls, Phys. Rev. A **56**, 833 (1997).

[5] P. Horak, G. Hechenblaikner, K. M. Gheri, H. Stecher, and H. Ritsch, Phys. Rev. Lett. **79**, 4979 (1997).

[6] G. Hechenblaikner,P. Gangl, P. Horak and H. Ritsch, Phys. Rev. A **58**, 3030 (1998).

[7] T. Fischer, P. Maunz, T. Puppe, P. W. H. Pinkse, and G. Rempe

[8] P. Domokos, P. Horak, and H. Ritsch, J. Phys. B., At. Mol. Opt. Phys. **34** (2001) 187198

[9] P. Domokos and H. Ritsch, Phys. Rev. Lett. **89**, 253003 (2002).

[10] W. Niedenzu, S. Schütz, H. Habibian, G. Morigi, and H. Ritsch, Phys. Rev. A **88**, 033830 (2013).

[11] P. Maunz, T. Puppe, I. Schuster, N. Syassen, P. W. H. Pinkse, and G. Rempe, Nature **428**, 50-51 (2004)

[12] C. J. Hood, T. W. Lynn, A. C. Doherty, A. S. Parkins, and H. J. Kimble Science **287**, 1447 (2000).

[13] P. W. H. Pinkse, T. Fischer, P. Maunz, and G. Rempe, Nature **404**, 365-368 (2000)

[14] B. L. Lev, A. Vukics, E. R. Hudson, B. C. Sawyer, P. Domokos, H. Ritsch, and J. Ye, Phys. Rev. A **77**, 023402 (2008).

[15] R. Schulze, C. Genes and H. Ritsch, Phys. Rev. A **81**, 063820 (2010).

[16] O. Romero-Isart, A. C. Pflanzer, M. L. Juan, R. Quidant, N. Kiesel, M. Aspelmeyer, and J. I. Cirac, Phys. Rev. A **83**, 013803 (2011).

[17] N. Kiesel, F. Blaser, U. Delic, D. Grass, R. Kaltenbaek and M. Aspelmeyer, PNAS, vol. 11, no. 35, 14180(2013).

[18] P. Asenbaum, S. Kuhn, S. Nimmrichter, U. Sezer and M. Arndt, Nat. Commun. **4**, 2743 (2013).

[19] M. Koch, C. Sames, A. Kubanek, M. Apel, M. Balbach, A. Ourjoumtsev, P. W. H. Pinkse, and G. Rempe, Phys. Rev. Lett. **105**, 173003 (2010)

[20] A. Kubanek, M. Koch, C. Sames, A. Ourjoumtsev, T. Wilk, P. W. H. Pinkse, and G. Rempe, Appl Phys B **102**, 433442 (2011)

[21] J. Struck, C. Ölschläger, M. Weinberg, P. Hauke, J. Simonet, A. Eckardt, M. Lewenstein, K. Sengstock, and P. Windpassinger, Phys. Rev. Lett. **108**, 225304, (2012).

[22] D. Bouwmeester, I. Marzoli, G. P. Karman, W. Schleich and J. P. Woerdman, Phys. Rev. A **61**, 013410(1999).

[23] W. Dür, R. Raussendorf, V. M. Kendon and H. J. Briegel, Phys. Rev. A **66**, 052319 (2002).

[24] B. C. Travaglione and G. J. Milburn, Phys. Rev. A **65**, 032310 (2002).

[25] A. Dantan, B. Nair, G. Pupillo and C. Genes, arxiv:1406.8420 (2014).

[26] H. Ritsch, P. Domokos, F. Brennecke, and T. Esslinger, Rev. Mod. Phys. **85**, 553 (2013).

[27] D. F. Walls and G. J. Milburn, Quantum Optics, Springer (1994).

[28] C. W. Gardiner, P. Zoller, Quantum Noise, Springer (2004)

[29] M. Aspelmeyer, T. J. Kippenberg, and F. Marquardt, arXiv:1303.0733 (2013)

[30] C. Genes, D. Vitali, P. Tombesi, S. Gigan, and M. Aspelmeyer, Phys. Rev. A **77**, 033804 (2008)

[31] C. Genes, H. Ritsch, and D. Vitali, Phys. Rev. A **80**, 061803(R) (2009)

[32] M. Barber, Random and Restricted Walks: Theory and Applications (Gordon and Breach, New York, NY, 1970), 1st ed.

[33] E. F. Fama, Financial Analysts Journal 21, **55** (1965)

[34] S. Redner, Non-Equilibrium Processes, Boston University (2007)

[35] M. Lax, W. Cai, and M. Xu, Random processes in physics and finance, Oxford University Press (2006)

[36] E. A. Codling, M. J. Plank, and S. Benhamou, J. R. Soc. Interface **5**, 813-834 (2008)

[37] A. J. McKane, Encyclopedia of Complexity and System Science, New York: Springer; p. 8766-8783 (2009)

[38] F. Verhulst, Perturbation analysis of parametric resonance, Encyclopedia of Complexity and Systems Science, Springer (2009)

[39] E. Butikov, Europ. J. o. Phys., v. **25**, No. 4, p.535-554 (July 2004)

[40] G. M. Zaslavsky, Physics of chaos in Hamiltonian systems, Imperial College Press (2007)

[41] B. Eckhardt, ”Chaos”, Fischer (2004)

[42] H. G. Schuster, Deterministic Chaos: an introduction, VCH (1995)

[43] A. Mertins, Signaltheorie, Vieweg-Teubner (2010)

[44] J. Kempe, Cont. Phys., Vol. **44** (4), p.307-327 (2003)

[45] Y. Aharonov, L. Davidovic, and N. Zagury, Phys. Rev. A, **48**, 1687 (1993)